Online ISSN : 2186-490X
Print ISSN : 1346-4272
CODEN : CCKHA7

地質調査研究報告

地質調査研究報告

BULLETIN OF THE GEOLOGICAL SURVEY OF JAPAN

Vol. 64 No. 11/12 2013

National Institute of Advanced Industrial Science and Technology
AIST

独立行政法人
産業技術総合研究所
地質調査総合センター

平成25年

Bulletin of the Geological Survey of Japan

Vol. 64, No. 11/12, P. 313–340 2013

地質調査研究報告
BULLETIN OF THE GEOLOGICAL SURVEY OF JAPAN
Vol. 64 No. 11/12 2013

論文

表紙の写真

産総研地下水等総合観測網の歪計の設置風景

（写真：板場智史）

Cover page

Installing a strainmeter of the integrated groundwater observation well network for earthquake prediction of the Geological Survey of Japan, AIST

(Photograph by Satoshi Itaba)

Bulletin of the Geological Survey of Japan, vol. 64 (11/12), p. 313 - 330, 2013

Article

Geochemical characteristics determined by multiple extraction from ion-adsorption type REE ores in Dingnan County of Jiangxi Province, South China

Kenzo Sanematsu[1],[2]* and Yoshiaki Kon[1]

Kenzo Sanematsu,(2013) Geochemical characteristics determined by multiple extraction from ion-adsorption type REE ores in Dingnan County of Jiangxi Province, South China. *Bull. Geol. Surv. Japan*, vol. 64 (11/12), p. 313-330, 5 figures, 5 tables, 1 appendix.

Abstract: This article reports results of the multiple six-step extraction and single step extraction experiments conducted on five ion-adsorption ores and three weathered granite samples collected from the Dingnan County in Jiangxi Province, China. The six-step extraction consists of ion-exchangeable (reacted with sodium acetate) fraction, organic-matter (sodium pyrophosphate) fraction, amorphous Fe oxide and Mn oxide (hydroxylamine at 30˚C) fraction, Fe and Mn oxides (hydroxylamine at 60 ˚C) fraction, clays-sulfide (aqua regia) fraction and silicates (mixture acid) fraction. The five ion-adsorption ores from a mining site contained the ion-exchangeable elements by sodium acetate solution ranging from 174 to 388 ppm REY (43 – 68 % relative to whole-rock contents), from 1.1 to 3.5 ppm Th (3.7 – 9.4 %) and from 0.44 to 1.0 ppm U (14 – 25 %). Concentrations of the extracted elements from the ores by ammonium sulfate solution (single step) range from 170 to 346 ppm REY (42 – 64 %), from 0.03 to 0.31 ppm Th (0.1 – 0.8 %) and from 0.25 to 0.71 ppm U (8 – 18 %). The ion-exchangeable fraction is remarkably depleted in Ce relative to the other REY, and is slightly depleted in HREE and Y, compared with the whole-rock compositions. Thorium is dominantly present in the organic-matter fraction, and is moderately contained in the clay-sulfide fraction and in residue. Uranium is extensively present in the residue, silicates fraction, ion-exchangeable fraction, clays-sulfides fraction, and organic-matter fraction. Results of three weathered granite samples outside of a mine are not significantly different although the REY contents or percentages of ion-exchangeable REY are lower than the ores.

Keywords: REE, Th, U, ion-adsorption ore, granite, weathering, adsorption, extraction, South China

1. Introduction

Rare earth elements (REE: La - Eu) can be classified into light REE (LREE: La - Eu) and heavy REE (HREE: Ga - Lu), and HREE-producing deposits are mostly confined to ion-adsorption type in the world (Roskill, 2011). The ion-adsorption type REE deposits have been economically mined in South China, consisting of weathered granite which is called an ion-adsorption ore. The ore grade is generally several hundred ppm and locally reaches up to 3800 ppm (Wu *et al*., 1990; Bao and Zhao, 2008). Since REE and Y (REY) are adsorbed on weathering products such as kaolin in the ore, they are extracted by ion-exchange with electrolyte solution like ammonium sulfate solution (Chi and Tian, 2009). The percentage of ion-exchangeable REY relative to the whole-rock grade is generally over 50% (Wu *et al*., 1990; Bao and Zhao, 2008; Chi and Tian, 2009).

Several publications have reported the results of extraction experiments on the ion-adsorption ores from South China (Wu *et al.*, 1990; Chi and Tian, 2009; Moldoveanu and Papangelakis 2012; 2013a), from Southeast Asia (Sanematsu *et al.*, 2009; 2013; Imai *et al*., 2013), and from Africa (Le Couteur, 2011; Moldoveanu and Papangelakis, 2013b). Wu *et al*. (1990) conducted extraction experiments and discussed the genesis of ion-adsorption ores. Chi and Tian (2009) summarized the extraction experiments and metallurgical process of the ores. Recently, Moldoveanu and Papangelakis (2012; 2013a) con-

[1] Institute for Geo-Resources and Environment, Geological Survey of Japan, National Institute of Advanced Industrial Science and Technology (AIST), Central 7, 1-1-1 Higashi, Tsukuba 305-8567, Japan. E-mail: k-sanematsu@aist.go.jp
[2] ARC Centre of Excellence in Ore Deposits (CODES), University of Tasmania, Private Bag 126, Hobart, Tasmania 7001, Australia
*Corresponding author: Kenzo Sanematsu

ducted the extraction experiments to compare the results in different reagents, pH, concentrations and temperatures. Their results suggest that LREE are more adsorbed than HREE and Y. Few previous works except Hoang *et al*. (1989) and Sanematsu *et al*. (2009; 2013) reported the REE-source minerals in the parent rocks. Mineral assemblage of the REE-bearing minerals is important because it strongly influences the fractionation of REE in the ore formation process (Hoang *et al*., 1989; Sanematsu *et al*., 2013). Considering the variety of ion-adsorption ores in different localities, specific geochemical data and mineralogical description are still insufficient to understand a proportion of ion-exchangeable REY, fractionation between LREE and HREE, and impurities in the extracted solutions. It is necessary to investigate the fractionation of REE, because HREE are more precious than LREE. Impurities, particularly Th and U, are not desirable in the extracted solutions.

In this article, we report the extraction results of the six-step and single step extraction experiments on five ion-adsorption ores from a REE mine and three weathered granite outside of the mine in South China, in order to discuss the geochemical characteristics of the ion-adsorption ores and extracted solutions. Residual REE-bearing minerals are also described using a SEM-EDS so that we can presume the REE-source minerals in the ores.

2. Geological background of the studied samples

The Phanerozoic igneous rocks are distributed in South China, and were formed by three major tectonic events: the Middle Paleozoic Kwangsian, Triassic Indosinian and Jurassic-Cretaceous Yanshanian events (e.g., Zhou *et al*., 2006; Wang *et al*., 2011; Zhang *et al*., 2012). The productive ion-adsorption type REE deposits were found in the Nanling Range of the Yanshanian granitoid area, however they are not common in the Kwangsian and Indosinian granitoid areas.

The Yanshanian magmatism is spatiotemporally related to metallogeny in South China, resulting from the southwestward subduction of the Pacific Plate and intraplate tectonics (Wang *et al.*, 2011). The Yanshanian period is divided into the Early Yanshanian (180 – 142 Ma) and Late Yanshanian (142 – 67 Ma) periods (Zhou *et al.*, 2006). Major REE deposits were found in the Early Yanshanian granite area rather than the Late Yanshanian one. The HREE-rich deposit area in the Early Yanshanian age is confined to the middle (southern Jiangxi and northern Guangdong) and south of the Nanling Range (Wu *et al*., 1992). Some of the Early Yanshanian granite plutons were formed by extensional rift-type intraplate magmatism, consisting of calc-alkaline granite, A-type granite, alkali granite, and syenite (Zhou *et al*., 2006; Guo *et al*., 2012). Parent granites of the ion-adsorption ores consist mainly of calc-alkaline granite and alkali granite based on the chemical compositions (Huang *et al*., 1989; Bao and Zhao, 2008; Ishihara *et al*., 2008).

3. Experimental and Analytical Methods

3.1 Sample descriptions

A total of eight weathered granite samples including ion-adsorption ores were selected from the previously studied samples of Murakami and Ishihara (2008). They were collected from weathering profiles of granite in Dingnan County, Jiangxi Province, China. Three samples of 1130S0 to 1130S2 (abbreviated to S0 – S2) were collected from a weathering profile outside of an ion-adsorption type deposit. Five samples of 1130S3 to 1130S7 (abbreviated to S3 – S7) are "ion-adsorption ores" taken from two different weathering profiles are collected from the ion-adsorption type deposit. These sampling locations are in the Early Yanshanian granite area (Murakami and Ishihara, 2008).

The weathered granite samples consist mainly of quartz, K-feldspar and kaolinite, and biotite and plagioclase were rarely identified by X-ray diffraction (Murakami and Ishihara, 2008). Whole-rock chemical compositions (REY, Th and U) of the studied samples are listed in Table 1.

3.2 Conditions of SEM-EDS

Polished mounts of ion-adsorption ores were prepared to observe the occurrences of REE-bearing minerals by using the JEOL JSM-6610LV scanning electron microscope. A qualitative and semi-quantitative analysis was performed by using the Oxford Instruments X-max energy dispersive X-ray spectroscopy system at an accelerating voltage of 15 kV.

3.3 Multiple six-step extraction

Multiple six-step extraction and single step extraction experiments were conducted on the pulverized weathered granite and ion-adsorption ore samples. The extraction experiments and ICP-MS analysis of extracted solutions were conducted in Activation Laboratories Ltd. Procedure of the six-step extraction is shown in Table 2. At the step 1, firstly, exchangeable ions were extracted by 1 M sodium acetate (CH_3COONa) solution of pH = 5 for 1 hour. At the step 2, elements were extracted predominantly by decomposing humic and fulvic acids with alkaline (pH = 10) 0.1 M sodium pyrophosphate ($Na_4P_2O_7$) solution for 1 hour. This alkaline solution may decompose silicate minerals because the solubility of silicate minerals is high in alkaline solution. At step 3, elements were extracted by predominantly leaching amorphous Fe oxides and Mn oxides with 1.24 M hydroxylamine (NH_2OH) at 30 ˚C for 2 hours. Because the hydroxylamine is a reducing agent, it may dissolve the solids

Table. 1 REY, Th and U contents of studied samples collected from Dingnan County of Jiangxi Province, South China (Murakami and Ishihara, 2008).

Sample #	Rock type	Depth (m)	Y (ppm)	La (ppm)	Ce (ppm)	Pr (ppm)	Nd (ppm)	Sm (ppm)	Eu (ppm)	Gd (ppm)	Tb (ppm)	Dy (ppm)	Ho (ppm)
1130S0	Weathered granite	0.3	64.9	42.4	100	7.62	28.7	6.83	0.45	7.54	1.53	10.6	2.15
1130S1	Weathered granite	0.6	71.2	78.6	235	13.7	49.3	10.1	0.65	10.8	1.85	11.6	2.31
1130S2	Weathered granite	1	59.5	79.0	205	13.4	48.4	9.82	0.59	9.51	1.56	9.68	1.89
1130S3	Ion-adsorption ore	0.25	49.8	48.7	204	10.1	42.4	10.1	1.99	9.58	1.73	10.1	1.89
1130S4	Ion-adsorption ore	0.1	56.6	126	149	26.0	102	20.0	3.28	17.1	2.39	12.6	2.19
1130S5	Ion-adsorption ore	0.3	46.0	58.9	207	12.7	51.6	10.5	1.91	9.66	1.48	8.54	1.60
1130S6	Ion-adsorption ore	0.1	62.0	96.8	172	22.2	92.0	18.3	2.98	15.6	2.18	11.8	2.14
1130S7	Ion-adsorption ore	0.2	62.3	113	300	22.8	89.5	17.6	2.82	15.3	2.18	11.7	2.06

Sample #	Er (ppm)	Tm (ppm)	Yb (ppm)	Lu (ppm)	Th (ppm)	U (ppm)	LREE (ppm)	HREE (ppm)	REE (ppm)	REY (ppm)	Ce/Ce*	Eu/Eu*	La_N/Yb_N
1130S0	6.30	0.993	6.13	0.835	49.9	5.4	186	36.1	222.1	287	1.36	0.19	4.96
1130S1	6.81	1.05	6.41	0.877	51.2	5.1	387	41.7	429.1	500	1.76	0.19	8.80
1130S2	5.46	0.834	4.98	0.692	51.3	4.8	356	34.6	390.8	450	1.54	0.19	11.4
1130S3	5.43	0.90	5.93	0.858	36.8	4.7	317	36.4	353.7	404	2.26	0.62	5.89
1130S4	6.11	0.907	5.80	0.828	30.2	3.2	426	47.9	474.2	531	0.64	0.54	15.6
1130S5	4.46	0.69	4.28	0.608	36.8	4.2	343	31.3	373.9	420	1.86	0.58	9.87
1130S6	5.81	0.851	5.15	0.709	34.2	3.8	404	44.2	448.5	511	0.91	0.54	13.5
1130S7	5.45	0.774	4.59	0.614	28.6	2.8	546	42.7	588.4	651	1.45	0.53	17.7

$Ce/Ce^* = Ce_N/(La_N \times Pr_N)^{1/2}$ and $Eu/Eu^* = Eu_N/(Sm_N \times Gd_N)^{1/2}$, where subscript N represents normalization by C1-chondrite (Sun and McDonough, 1989).

Table. 2 Experimental conditions of the multiple six-step extraction. The series of these experiments were conducted in Activation Laboratories Ltd. in Vancouver, Canada.

Extraction step #	Reagent	pH	Reaction time (hrs)	Dominantly reacting materials
1	1M sodium acetate	5	1	Ion-exchangeable materials
2	0.1M sodium pyrophosphate	10	1	Organic matter (humic and fulvic substances)
3	1.24M hydroxylamine (30℃)	1	2	Amorphous Fe oxide and Mn oxide
4	1.24M hydroxylamine (60℃)	1	2	Fe and Mn oxides
5	Aqua regia	-	2	Clays and sulfides
6	Mixture acid (HF, HNO_3, $HClO_4$ and HCl)	-	19	Acid-soluble silicates and remaining materials

whose solubilities are high in reduced conditions. At step 4, elements were extracted by leaching remaining crystalline Fe and Mn oxides with 1.24 M hydroxylamine at 30 ˚C for 2 hours. At the step 5, elements incorporated in clays, sulfides and some remaining materials were leached by aqua regia for 2 hours. Because the aqua regia is an oxidizing agent, it may dissolve the solids whose solubilities are high in oxidized conditions. Lastly, at the step 6, elements incorporated in silicates and some remaining materials were leached by mixture acid consisting of HF, HNO_3, $HClO_4$ and HCl after 19-hours reaction. We are able to estimate the dominantly-reacted materials from the results of the individual extraction steps, however it is generally difficult to clarify the reacted materials and to know whether the materials are reacted completely.

3.4 Single-step extraction

In order to check the concentrations of ion-exchangeable elements using a different electrolyte solution, a single step extraction and solution ICP-MS analysis were done by authors in Geological Survey of Japan, AIST. Procedure of the single-step extraction is shown in Table 3. Weathered granite samples were pulverized by an agate mortar and were dried at 105 ˚C

Table. 3 Experimental condition of the single step extraction using ammonium sulfate solution.

Extraction step #	Reagent	pH	Reaction time (hrs)	Dominantly reacting materials
1	0.5M ammonium sulphate	5.7	24	Ion-exchangeable materials

for 12 hours to evaporate water. The individual samples of 1 g was soaked in 40 ml volume of 0.5 M (6.6 wt%) ammonium sulfate [$(NH_4)_2SO_4$] solution of pH = ~5.7 in a 50 ml centrifuge tube. The centrifuge tubes were mechanically shaken at room temperature for 24 hours so that the solid sample can react with solution sufficiently. The extract was separated from the solid samples by centrifugation for 15 minutes. The supernatant solution was filtered by using a cellulose acetate-type membrane filter (φ=0.22 μm), and the membrane filter was rinsed repeatedly with 50 ml of ultra pure water. The filtered solution was acidified using HNO_3 and was kept in a polypropylene container. Ultra pure water and In standard solution (Wako) as an internal standard was added to the acidified sample solution, and it was prepared to 1 % HNO_3 equivalent before analysis.

Concentrations of extracted elements at the single step extraction were determined by the Agilent Technologies 7500cx ICP-MS at the Geological Survey of Japan, AIST. Flow rates of carrier gas and the ion-lens setting of the ICP-MS were optimized to maximize the signal intensity of Ce and to minimize the oxide production rate ($^{140}Ce^{16}O/^{140}Ce < 0.01$). We monitored ^{7}Li, ^{23}Na, ^{24}Mg, ^{27}Al, ^{29}Si, ^{31}P, ^{39}K, ^{43}Ca, ^{45}Sc, ^{47}Ti, ^{51}V, ^{53}Cr, ^{55}Mn, ^{57}Fe, ^{59}Co, ^{60}Ni, ^{63}Cu,^{66}Zn, ^{69}Ga, ^{72}Ge, ^{75}As, ^{85}Rb, ^{88}Sr, ^{89}Y, ^{90}Zr, ^{93}Nb, ^{95}Mo, ^{107}Ag, ^{111}Cd, ^{115}In (internal standard), ^{133}Cs, ^{137}Ba, ^{139}La, ^{140}Ce, ^{141}Pr, ^{146}Nd, ^{147}Sm, ^{153}Eu, ^{157}Gd, ^{159}Tb, ^{163}Dy, ^{165}Ho, ^{166}Er, ^{169}Tm, ^{172}Yb, ^{175}Lu, ^{181}Ta, ^{182}W, ^{205}Tl, ^{208}Pb, ^{209}Bi, ^{232}Th and ^{238}U. Calibration lines were made by multi-element standard solutions of XSTC-1, -8 and -15 (SPEX). The combination of analogue and pulse-counting mode of the ICP-MS was used for monitoring the minor elements and the detector mode was switched to the analog-counting mode automatically when abundant elements were monitored.

4. Results

4.1 Results of SEM-EDS

Backscattered electron images of residual or secondary REE-bearing minerals are shown in Figure 1. Zircon ($ZrSiO_4$) is the most common REE-bearing mineral in the studied ion-adsorption ores. It is rarely altered and the grain size ranges from 10 to 100 μm (Fig. 1A, 1B, 1C and 1F). Thorium silicate ($ThSiO_4$: thorite or huttonite) is partly found (Fig. 1B). Monazite-(Ce) [$(Ce,Th)PO_4$] is relatively uncommon and this is not significantly altered (Fig. 1D and 1E). Apatite [$Ca_5(PO_4)_3(F,Cl)$] is uncommon as well and is partly weathered and degraded (Fig. 1F). Xenotime (YPO_4) is more scarce than monazite and apatite. REE phosphate-silicate is found (Fig. 1F and 1G) and is likely britholite-(Ce) [$(Ce,Ca,Th)(SiO_4,PO_4)(OH,F)$]. REE fluorocarbonates are partly observed and they are considered to be synchysite-(Ce) [$CaCe(CO_3)_2F$], parasite-(Ce) [$CaCe_2(CO_3)_3F_2$] and/or bastnasite-(Ce) [$Ce(CO_3)F$]. These carbonates exhibit fine-grained (<20 μm) anhedral shape and occur in the cavities and fractures in K-feldspar. K-feldspar is partly or wholly kaolinitized (Fig. 1H and 1I). Secondary REE-bearing minerals consist of CeO_2 and Mn oxy-hydroxide. They are enriched in Ce(IV) but other REE(III) are rarely incorporated in these materials. CeO_2 is considered to Th-poor cerianite (if it is crystalline) and occurs as aggregates of fine-grained particles. The aggregates of CeO_2 are commonly found with kaolinite, K-feldspar or Mn oxy-hydroxide (Fig. 1K and 1J). Ce-bearing Mn oxy-hydroxide occurs as aggregates of platy crystals (Fig. 1J) or exhibits dendritic texture (Fig. 1L).

4.2 Results of extraction experiments

Results of the extraction experiments are summarized in Tables 4 and 5, and individual element data are presented in Appendix. Percentages of extracted REY, Th and U relative to whole-rock contents are show in Figures 2, 3 and 4, respectively. Results of the six-step extraction indicate that REY were extracted predominantly from the ion-exchangeable fraction (step 1) and from the organic-matter fraction (step 2) in most of the samples (Fig. 2). The other fractions were relatively poor in REY although the Fe-Mn-oxides fractions (steps 3 and 4) were rich in Ce. Thorium was extracted predominantly from the organic-matter fraction and from the clays-sulfides fraction (step 5), and was present in a residual fraction (Fig. 3). The residual fraction was estimated by subtracting the extracted concentrations (step 1 to step 6) from the whole-rock contents (Table 4). Negative values of the residual fraction in the weathered granite (S0, S1 and S2) and ion-adsorption ore (S6) were attributed to sampling the heterogeneous portions between the whole-rock analysis and extraction experiment. Uranium was extracted from the ion-exchangeable fraction, organic-matter fraction, Fe-Mn-oxides fractions, clays-sulfides fraction and silicates fraction, and was also present in the residual fraction.

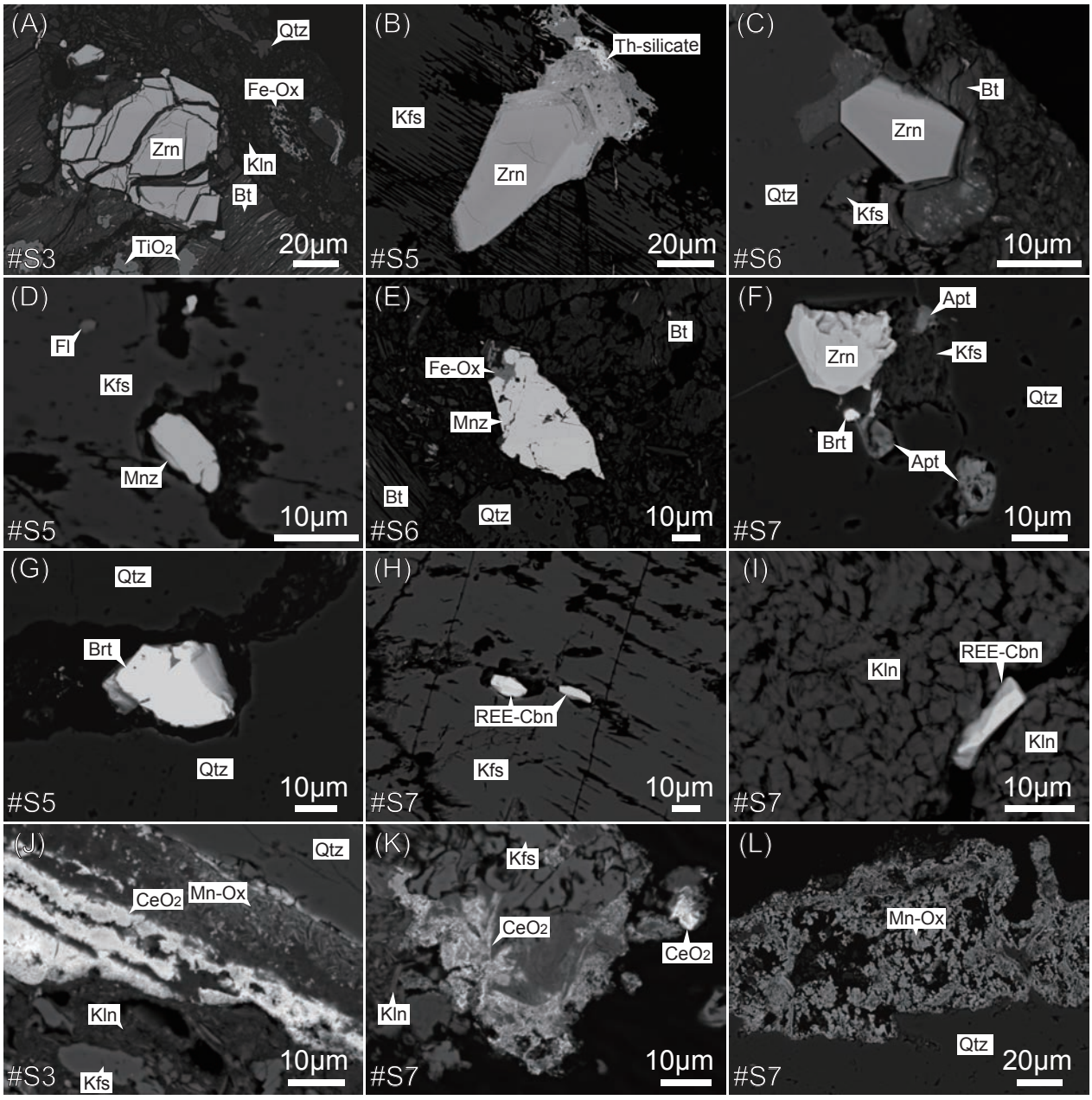

Fig. 1 Backscattered electron images of the ion-adsorption ores. The residual REE-bearing minerals consist mainly of (A, B, C) zircon with lesser amounts of (D, E) monazite-(Ce), (F) apatite, (G) britholite-(Ce) and (H, I) REE fluorocarbonates. The secondary Ce-bearing minerals consist of (J, K) CeO2 (probably cerianite) and (J, L) Mn oxyhydroxide. Sample numbers (#s) are shown on the individual images. Abbreviations: Zrn, zircon; Kln, kaolinite; Qtz, quartz; Fe-Ox, Fe oxyhydroxide; Bt, biotite; Kfs, K-feldspar; Mnz, monazite-(Ce); Fl, fluorite; Apt, apatite; Brt, britholite-(Ce); REE-Cbn, REE fluorocarbonate-(Ce); Mn-Ox, Mn oxyhydroxide.

4.2.1 Ion-exchangeable fraction

Concentrations of the extracted elements from the five ion-adsorption ores by sodium acetate solution (step 1) range from 174 to 388 ppm REY (43 – 68 % relative to whole-rock contents; the same shall apply hereafter), from 1.1 to 3.5 ppm Th (3.7 – 9.4 %) and from 0.44 to 1.0 ppm U (14 – 25 %). Concentrations of the extracted elements from the ores by ammonium sulfate solution (single step) range from 170 to 346 ppm REY (42 – 64 %), from 0.03 to 0.31 ppm Th (0.1 – 0.8 %) and from 0.25 to 0.71 ppm U (8 – 18 %).

Concentrations of the extracted elements from the three weathered granite samples by sodium acetate solution (step 1)

Table. 4 Results of the six-step extraction experiment. The other elements are listed in Appendix. Note that negative values of the estimated residual fraction are attributed to sampling the heterogeneous portions between the whole-rock analysis and extraction experiment. See Table 2 for the experimental conditions.

Sample		Fraction	LREE		HREE		REE		Y		REY		Th		U		Ce/Ce*	Eu/Eu*	La_N/Yb_N
			(ppm)	(%)	(ppm)	(%)	(ppm)	(%)	(ppm)	(%)	(ppm)	(%)	(ppm)	(%)	(ppm)	(%)			
Weathered granite	S0	Ion-exchangeable (Na acetate)	76.7	41.2	12.8	35.4	89	40.3	20.3	31.3	110	38.2	3.3	6.7	0.85	15.7	0.35	0.16	15.7
		Organic matter	107	57.3	2.3	6.4	109	49.0	2.8	4.3	112	38.9	22.3	44.7	0.7	12.9	13.3	0.13	10.4
		Amorphous Fe-Ox & Mn-Ox	8.9	4.8	0.34	0.94	9.2	4.2	0.49	0.7	9.7	3.4	0.14	0.3	0.05	0.9	6.6	0.16	12.7
		Fe and Mn oxides	20.5	11.0	0.19	0.52	20.7	9.3	0.16	0.2	20.9	7.3	0.11	0.2	0.07	1.3	15.2	0.14	13.8
		Clays and sulfides	4.8	2.6	1.2	3.4	6.0	2.7	2.0	3.1	8.0	2.8	11.5	23.0	0.7	12.9	1.8	n.d.	2.9
		Silicates	4.4	2.3	3.4	9.4	7.8	3.5	4.3	6.6	12.1	4.2	2.8	5.6	1.2	22.2	1.2	0.62	0.81
		Estimated residual	*-36*	*-19*	*16*	*44*	*-20*	*-9.0*	*35*	*54*	*15*	*5.2*	*9.7*	*19*	*1.8*	*34*	*n.d.*	*n.d.*	*n.d.*
		Whole-rock content	186	100	36	100	222	100	65	100	287	100	50	100	5.4	100	1.4	0.19	5.0
Weathered granite	S1	Ion-exchangeable (Na acetate)	173	44.6	21.1	50.7	194	45	30.4	43	224	44.8	3.6	7.0	0.94	18.3	0.32	0.16	26.5
		Organic matter	163	42.2	3.4	8.2	167	39	4.0	5.6	171	34.1	27.6	53.9	0.8	15.7	10.8	0.12	16.1
		Amorphous Fe-Ox & Mn-Ox	13.2	3.4	0.48	1.1	13.7	3.2	0.61	0.9	14.3	2.9	0.20	0.4	0.05	1.0	5.6	0.18	17.7
		Fe and Mn oxides	31.5	8.1	0.25	0.60	31.8	7.4	0.17	0.2	31.9	6.4	0.13	0.3	0.09	1.7	15.5	0.14	16.6
		Clays and sulfides	4.7	1.2	1.1	2.6	5.8	1.4	1.7	2.3	7.4	1.5	10.8	21	0.7	13.7	3.3	n.d.	2.2
		Silicates	5.5	1.4	3.1	7.4	8.6	2.0	5.3	7.4	13.9	2.8	2.9	5.7	1.3	25.5	1.1	0.75	1.2
		Estimated residual	*-3.5*	*-0.9*	*12*	*29*	*8.7*	*2.0*	*29*	*41*	*38*	*7.6*	*6.0*	*12*	*1.2*	*24*	*n.d.*	*n.d.*	*n.d.*
		Whole-rock content	387	100	41.7	100	429	100	71.2	100	500	100	51.2	100	5.1	100	1.8	0.19	8.8
Weathered granite	S2	Ion-exchangeable (Na acetate)	208	58.4	20.1	58.2	228	58.4	26.7	44.9	255	56.6	5.4	10.6	1.2	24.3	0.57	0.16	28.7
		Organic matter	133	37.4	3.4	9.9	137	35.0	4.4	7.3	141	31.3	23.2	45.2	0.8	16.8	6.5	0.13	20.3
		Amorphous Fe-Ox & Mn-Ox	7.6	2.1	0.35	1.0	7.9	2.0	0.43	0.7	8.4	1.9	0.16	0.3	0.04	0.9	3.6	0.27	19.1
		Fe and Mn oxides	17.6	4.9	0.23	0.67	17.8	4.6	0.22	0.4	18.0	4.0	0.10	0.2	0.06	1.3	8.4	0.18	19.5
		Clays and sulfides	4.2	1.2	1.5	4.3	5.7	1.4	2.4	4.0	8.1	1.8	8.8	17.2	0.8	16.8	1.1	n.d.	2.4
		Silicates	6.0	1.7	3.3	9.5	9.3	2.4	5.1	8.6	14.4	3.2	3.9	7.6	1.2	25.2	1.0	0.53	1.3
		Estimated residual	*-20*	*-5.7*	*5.7*	*16*	*-15*	*-3.8*	*20*	*34*	*5.6*	*1.2*	*9.7*	*19*	*0.7*	*15*	*n.d.*	*n.d.*	*n.d.*
		Whole-rock content	356	100	34.6	100	391	100	59.5	100	450	100	51.3	100	4.8	100	1.5	0.19	11.4
Ion-adsorption ore	S3	Ion-exchangeable (Na acetate)	119	37.5	24.1	66.3	143	40.5	30.5	61.2	174	43.0	3.2	8.7	0.71	15.3	0.57	0.51	8.4
		Organic matter	112	35.4	4.3	11.8	117	33.0	4.3	8.6	121	30.0	13.3	36.1	0.4	8.6	8.9	0.47	6.2
		Amorphous Fe-Ox & Mn-Ox	18.0	5.7	0.86	2.4	18.9	5.3	0.86	1.7	19.7	4.9	0.18	0.5	0.03	0.7	7.2	0.49	7.0
		Fe and Mn oxides	24.1	7.6	0.39	1.1	24.4	6.9	0.35	0.7	24.8	6.1	0.05	0.1	0.05	1.0	11	0.45	8.0
		Clays and sulfides	11.9	3.8	1.4	3.8	13.3	3.8	1.7	3.5	15.0	3.7	6.2	16.8	0.8	17.2	1.1	n.d.	6.7
		Silicates	13.6	4.3	2.1	5.8	15.7	4.4	2.7	5.4	18.4	4.6	2.7	7.3	1.0	21.5	0.62	0.89	5.6
		Estimated residual	*18*	*5.7*	*3.3*	*8.9*	*21*	*6.1*	*9.4*	*19*	*31*	*7.7*	*11.2*	*30*	*1.7*	*36*	*n.d.*	*n.d.*	*n.d.*
		Whole-rock content	317	100	36.4	100	354	100	49.8	100	404	100	36.8	100	4.7	100	2.3	0.6	5.9
Ion-adsorption ore	S4	Ion-exchangeable (Na acetate)	243	57.0	34.3	71.7	277	58.5	38.0	67.9	315	59.5	1.1	3.7	0.45	13.8	0.05	0.49	26.0
		Organic matter	94	22.1	4.7	9.9	99.0	20.9	4.8	8.6	104	19.6	11.4	37.7	0.2	6.2	3.91	0.50	11.3
		Amorphous Fe-Ox & Mn-Ox	17.1	4.0	1.4	2.9	18.5	3.9	1.5	2.7	20.0	3.8	0.17	0.6	0.04	1.3	1.83	0.51	13.3
		Fe and Mn oxides	35.8	8.4	0.82	1.7	36.6	7.7	0.70	1.2	37.3	7.0	0.09	0.3	0.06	1.9	5.09	0.47	12.3
		Clays and sulfides	17.5	4.1	2.5	5.1	19.9	4.2	2.3	4.1	22.2	4.2	10.4	34.4	0.7	21.7	0.63	0.41	9.9
		Silicates	2.7	0.6	0.8	1.7	3.5	0.7	0.70	1.3	4.2	0.8	0.40	1.3	0.5	15.5	0.49	n.d.	1.9
		Estimated residual	*15.9*	*3.7*	*3.4*	*7.1*	*19*	*4.1*	*8.0*	*14*	*27*	*5.1*	*6.6*	*22*	*1.3*	*40*	*n.d.*	*n.d.*	*n.d.*
		Whole-rock content	426	100	47.9	100	474	100	56.0	100	530	100	30.2	100	3.2	100	0.64	0.54	15.6
Ion-adsorption ore	S5	Ion-exchangeable (Na acetate)	173	50.5	20.4	65.1	193	51.7	24.6	53.5	218	51.9	3.5	9.4	1.03	24.7	0.56	0.45	21.1
		Organic matter	124	36.1	3.5	11.2	127	34.0	3.9	8.4	131	31.2	17.7	48.1	0.8	19.2	7.7	0.44	13.3
		Amorphous Fe-Ox & Mn-Ox	15.8	4.6	0.54	1.7	16.3	4.4	0.56	1.2	16.9	4.0	0.15	0.4	0.06	1.4	6.7	0.44	13.6
		Fe and Mn oxides	17.4	5.1	0.23	0.75	17.7	4.7	0.19	0.4	17.9	4.3	0.06	0.2	0.07	1.8	10	0.41	14.8
		Clays and sulfides	11.7	3.4	1.0	3.2	12.7	3.4	1.1	2.3	13.8	3.3	7.4	20.1	0.4	9.6	1.2	n.d.	9.3
		Silicates	5.4	1.6	1.3	4.2	6.7	1.8	1.9	4.1	8.6	2.1	1.1	3.0	0.5	12.0	0.88	1.68	2.7
		Estimated residual	*-4.3*	*-1.3*	*4.4*	*14.0*	*0.1*	*0.0*	*14*	*30*	*14*	*3.3*	*6.9*	*19*	*1.3*	*31*	*n.d.*	*n.d.*	*n.d.*
		Whole-rock content	343	100	31.3	100	374	100	46.0	100	420	100	36.8	100	4.2	100	1.9	0.58	9.9
Ion-adsorption ore	S6	Ion-exchangeable (Na acetate)	268	66.3	37.0	84	305	68.0	43.4	70.0	349	68.3	3.0	8.7	0.90	23.9	0.24	0.46	22.0
		Organic matter	113	27.9	4.0	9.1	117	26.0	4.9	7.8	122	23.8	16.1	47.1	0.6	15.9	5.1	0.46	15.3
		Amorphous Fe-Ox & Mn-Ox	14.3	3.5	0.66	1.5	14.9	3.3	0.74	1.2	15.7	3.1	0.23	0.7	0.05	1.4	4.1	0.41	15.1
		Fe and Mn oxides	21.4	5.3	0.30	0.68	21.7	4.8	0.25	0.4	21.9	4.3	0.07	0.2	0.08	2.2	8.2	0.37	14.8
		Clays and sulfides	12.3	3.0	1.0	2.3	13.3	3.0	1.4	2.2	14.7	2.9	8.2	24.0	0.5	13.2	1.3	n.d.	9.3
		Silicates	8.4	2.1	2.0	4.5	10.4	2.3	2.8	4.5	13.2	2.6	2.1	6.1	0.8	21.2	1.0	1.8	2.6
		Estimated residual	*-33*	*-8*	*-0.8*	*-1.7*	*-34*	*-7.5*	*8.6*	*14*	*-25*	*-4.9*	*4.5*	*13*	*0.8*	*22*	*n.d.*	*n.d.*	*n.d.*
		Whole-rock content	404	100	44	100	449	100	62.0	100	511	100	34.2	100	3.8	100	0.91	0.54	13.5
Ion-adsorption ore	S7	Ion-exchangeable (Na acetate)	298	54.5	39.3	92.1	337	57.3	51.0	81.9	388	59.6	1.7	5.9	0.44	15.8	0.11	0.45	30.3
		Organic matter	66.9	12.3	3.2	7.5	70.1	11.9	4.3	6.8	74.3	11.4	9.1	31.8	0.3	10.7	3.0	0.46	19.5
		Amorphous Fe-Ox & Mn-Ox	26.5	4.9	1.1	2.6	27.6	4.7	1.3	2.1	28.9	4.4	0.27	0.9	0.08	2.8	4.3	0.43	19.0
		Fe and Mn oxides	86.0	15.8	0.65	1.5	86.7	14.7	0.32	0.5	87.0	13.4	0.17	0.6	0.12	4.3	17.0	0.34	17.0
		Clays and sulfides	16.9	3.1	1.3	3.0	18.1	3.1	1.6	2.6	19.8	3.0	10.7	37.4	0.5	17.8	5.8	n.d.	2.9
		Silicates	4.3	0.8	1.7	4.0	6.0	1.0	2.0	3.2	8.0	1.2	1.2	4.2	0.7	24.9	1.4	2.3	0.96
		Estimated residual	*48*	*8.7*	*-4.5*	*-11*	*43*	*7.3*	*1.8*	*2.9*	*45*	*6.9*	*5.5*	*19*	*0.7*	*24*	*n.d.*	*n.d.*	*n.d.*
		Whole-rock content	546	100	42.7	100	588	100	62.3	100	651	100	28.6	100	2.8	100	1.45	0.53	17.7

$Ce/Ce^* = Ce_N/(La_N \times Pr_N)^{1/2}$, $Eu/Eu^* = Eu_N/(Sm_N \times Gd_N)^{1/2}$, where subscript N represents normalization by C1-chondrite (Sun and McDonough, 1989).
Whole-rock content data are from Murakami and Ishihara (2008). n.d., Not determined.

Table. 5 Results of the single step extraction showing extracted element concentrations (ppm) and percentages (%) to the whole-rock contents. The other elements are listed in Appendix. See Tables 3 for the experimental conditions.

	Sample	Fraction	LREE (ppm)	LREE (%)	HREE (ppm)	HREE (%)	REE (ppm)	REE (%)	Y (ppm)	Y (%)	REY (ppm)	REY (%)	Th (ppm)	Th (%)	U (ppm)	U (%)	Ce/Ce*	Eu/Eu*	La_N/Yb_N
Weathered granite	S0	Ion-exchangeable (ammonium sulfate)	73.3	39.4	11.6	32.1	84.8	38.2	18.4	28.3	103	36.0	0.23	0.45	0.55	10.1	0.38	0.16	17.2
	S1	Ion-exchangeable (ammonium sulfate)	160	41.2	19.3	46.2	179	41.7	28.7	40.4	208	41.5	0.17	0.33	0.64	12.5	0.35	0.15	26.9
	S2	Ion-exchangeable (ammonium sulfate)	187	52.5	18.3	52.9	205	52.5	26.0	43.6	231	51.4	0.34	0.67	0.83	17.4	0.58	0.15	28.8
Ion-adsorption ore	S3	Ion-exchangeable (ammonium sulfate)	119	37.6	22.1	60.8	141	40.0	28.5	57.3	170	42.1	0.25	0.68	0.37	7.9	0.70	0.48	9.4
	S4	Ion-exchangeable (ammonium sulfate)	220	51.6	30.9	64.4	251	52.9	35.6	63.5	286	54.0	0.03	0.10	0.25	7.7	0.06	0.48	26.5
	S5	Ion-exchangeable (ammonium sulfate)	163	47.7	18.3	58.6	182	48.6	23.5	51.2	205	48.9	0.31	0.84	0.71	17.1	0.63	0.45	21.5
	S6	Ion-exchangeable (ammonium sulfate)	256	63.3	34.4	77.8	290	64.7	35.1	56.6	325	63.7	0.20	0.57	0.66	17.5	0.26	0.45	22.0
	S7	Ion-exchangeable (ammonium sulfate)	270	49.4	36.6	85.7	306	52.1	39.5	63.4	346	53.1	0.12	0.41	0.35	12.4	0.12	0.44	29.6

$Ce/Ce^* = Ce_N/(La_N \times Pr_N)^{1/2}$, $Eu/Eu^* = Eu_N/(Sm_N \times Gd_N)^{1/2}$, where subscript N represents normalization by C1-chondrite (Sun and McDonough, 1989).

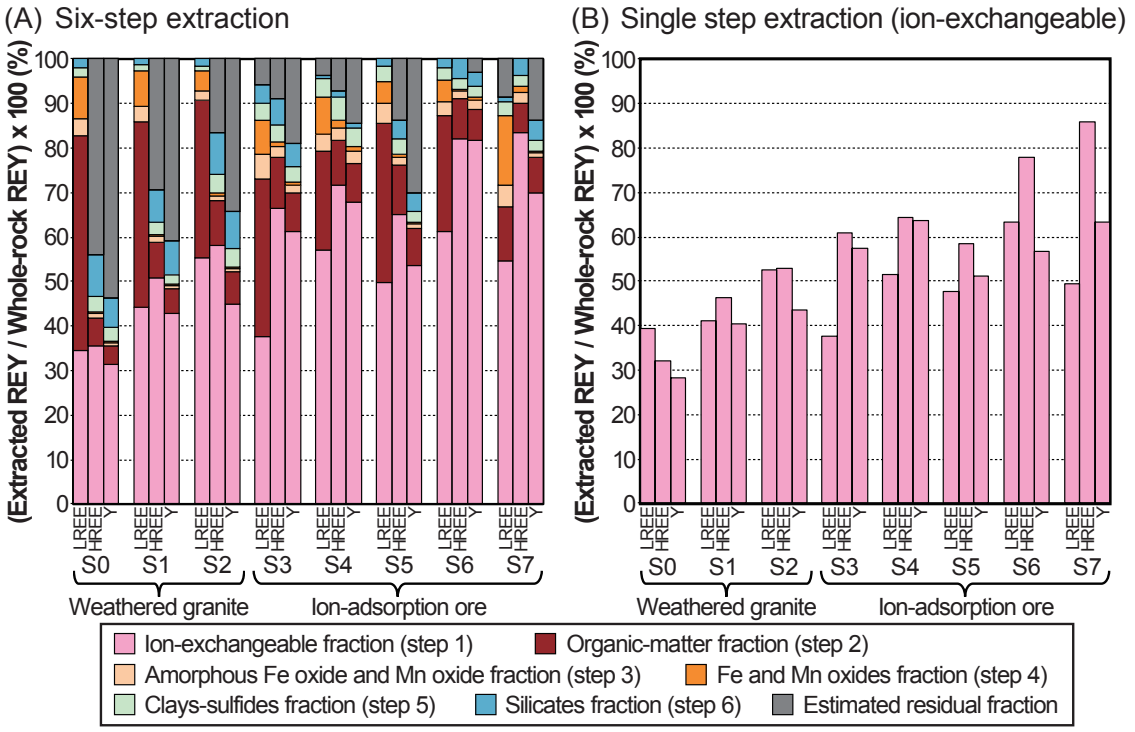

Fig. 2 (A) Percentages of extracted LREE, HREE and Y concentrations relative to their whole-rock contents, determined by the results of (A) the six-step extraction and (B) single step extraction. See Tables 2 and 3 for the experimental conditions. Note that the multiple-extraction columns with total concentrations exceeding 100 % are forcibly corrected to 100 % in total.

range from 110 to 255 ppm REY (38 – 57 %), from 3.3 to 5.4 ppm Th (6.7 – 11 %) and from 0.85 to 1.2 ppm U (16 – 24 %). Concentrations of the extracted elements from the weathered granites by ammonium sulfate solution (single step) range from 103 to 231 ppm REY (36 – 51 %), from 0.17 to 0.34 ppm Th (0.3 – 0.7 %) and from 0.5 to 0.8 ppm U (10 – 17 %).

Depletion of Ce is significant in the ion-exchangeable fraction and is represented by negative Ce anomalies ($Ce/Ce^* = Ce_N/(La_N \times Pr_N)^{1/2} = 0.05 – 0.57$, where the subscript N represents normalization by C1-chondrite hereafter; Sun and McDonough, 1989). Percentages of extracted Ce concentrations relative to the whole-rock contents are less than 35 %. La_N/Yb_N ratios, which indicate the fractionation between LREE and HREE, in ion-exchangeable fraction range from 8.4 to 30 in all the samples.

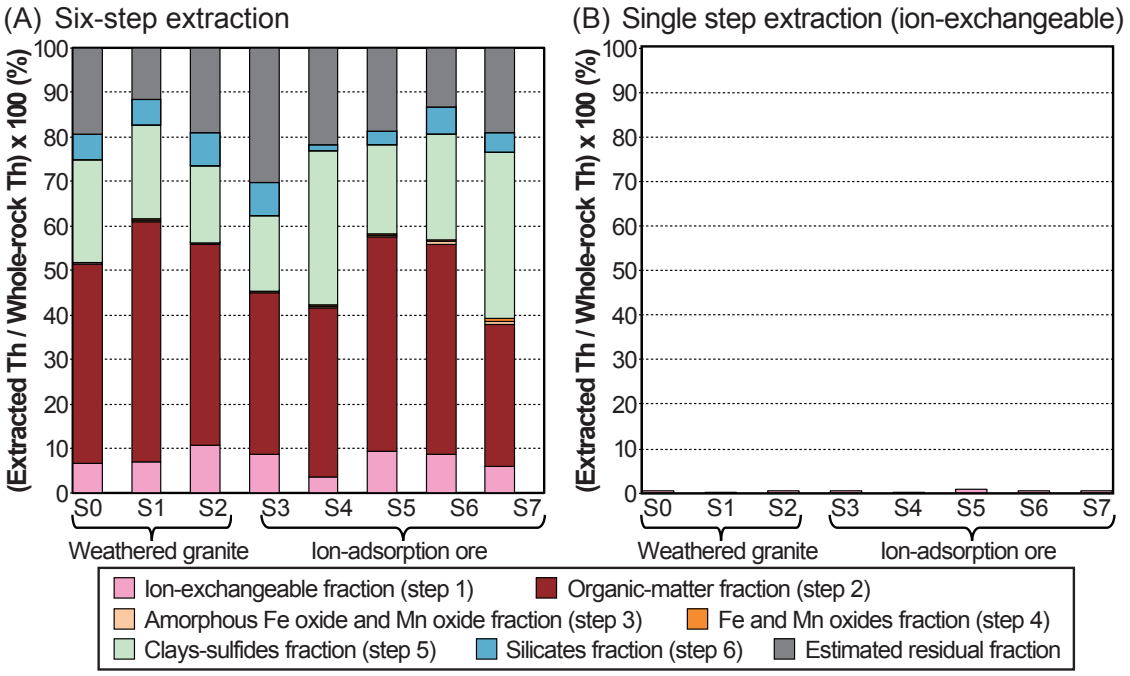

Fig. 3 Percentages of extracted Th concentrations relative to the whole-rock Th contents, determined by the results of (A) the six-step extraction and (B) single step extraction. See Tables 2 and 3 for the experimental conditions.

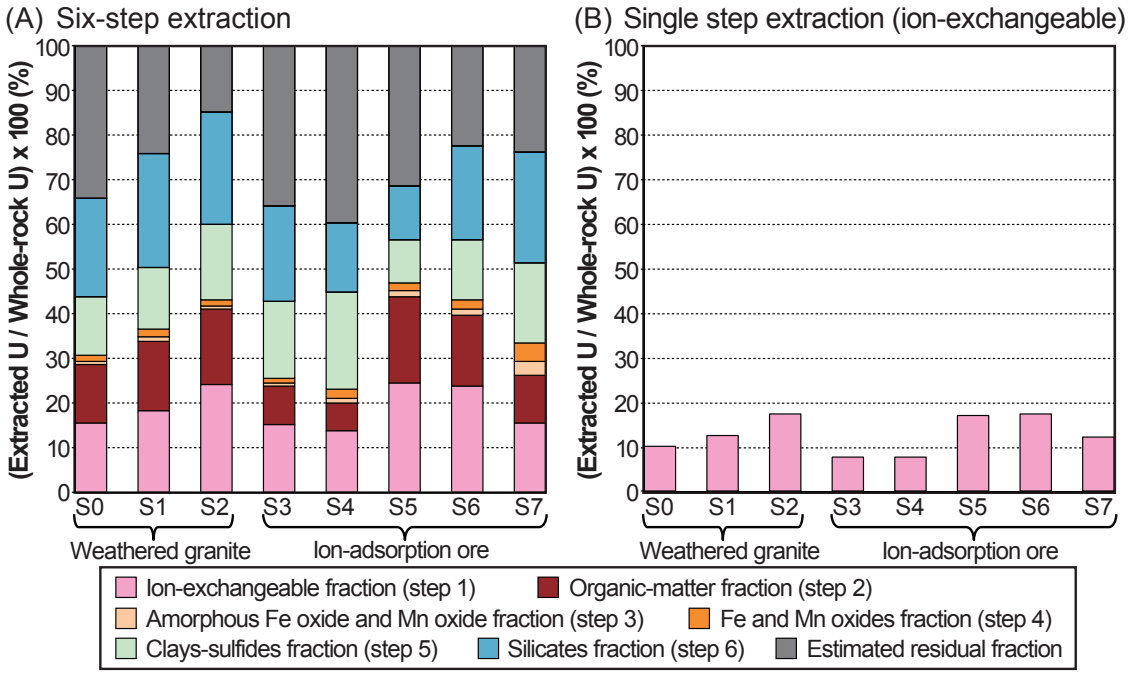

Fig. 4 Results of the sequential extraction showing percentages of extracted U concentrations relative to their whole-rock U contents, determined by the results of (A) the six-step extraction and (B) single step extraction. See Tables 2 and 3 for the experimental conditions.

4.2.2 Organic-matter fraction

In the organic-matter fraction (step 2), concentrations of extracted elements from ion-adsorption ores range from 74 to 131 ppm REY (11 – 31 %), from 9.1 to 18 ppm Th (32 – 48 %) and from 0.2 to 0.8 ppm U (6 – 19 %). Concentrations of extracted elements from weathered granite samples range from 112 to 171 ppm REY (31 – 39 %), from 22 to 28 ppm Th (45 – 54 %) and from 0.7 to 0.8 ppm U (13 – 17 %). All the samples show positive Ce anomalies (Ce/Ce* = 3.0 – 13) and La_N/Yb_N ratios ranging from 6.2 to 20.

4.2.3 Fe-Mn-oxides fraction

Concentrations of REY, Th and U extracted in Fe-Mn-oxides fractions (steps 3 and 4) of all the samples are lower than the first two fractions (steps 1 and 2) except for Ce (Table 4). Cerium is enriched in the steps 3 and 4, showing positive Ce anomalies (Ce/Ce* = 1.8 - 17). La_N/Yb_N ratios range from 7.0 to 20. Results of the step 4 (reaction temperature 60 ˚C) give higher concentrations of REY and U and lower concentrations of Th than those of the step 3 (reaction temperature 30 ˚C).

4.2.4 Clays-sulfides fraction

In the clays-sulfides fraction leached by aqua regia (step 5), the ion-adsorption ores show the element concentrations ranging from 14 to 22 ppm REY (3 – 4 %), from 6.2 to 11 ppm Th (17 – 37 %) and from 0.4 to 0.8 ppm U (10 – 22 %). The weathered granites show the element concentrations ranging from 7.4 to 8.1 ppm REY (1 – 3 %), from 8.8 to 12 ppm Th (17 – 23 %) and from 0.7 to 0.8 ppm U (13 – 17 %). La_N/Yb_N ratios range from 2.2 to 9.9, and they are significantly lower than the previous fractions of the extraction steps 1 – 4 in most of the samples.

4.2.5 Silicates fraction

The last step of the six-step extraction is the silicates fraction leached by mixture acid (step 6). Ion-adsorption ores show the concentrations of leached elements ranging from 4 to 18 ppm REY (1 – 5 %), from 0.4 to 2.7 ppm Th (1 – 7 %) and from 0.5 to 1.0 ppm U (12 – 22 %). Weathered granites show the concentrations of leached elements ranging from 12 to 14 ppm REY (3 – 4 %), from 2.8 to 3.9 ppm Th (6 – 8 %) and from 1.2 to 1.3 ppm U (22 – 25 %). Eu anomalies (Eu/Eu* = 0.53 – 2.3 except the sample S3) are significantly higher than those of the other fractions. La_N/Yb_N ratios range from 0.81 to 5.6, and they are lower than the ratios of the other fractions.

5. Discussion

5.1 REE and Y in ion-adsorption ores

Extracted REY concentrations by ammonium sulfate solution (pH = 5.7) are systematically lower than those by sodium acetate solution (pH = 5.0). This difference in the extracted concentrations is attributed to the differences in ion-exchangeable reagents, solution pH and/or drying temperatures before the experiments. An experimental study indicated that REY are more exchanged by NH_4^+ than by Na^+ from ion-adsorption ores (Moldoveanu and Papangelakis, 2012). This is inconsistent with our extraction results (Fig. 3; Table 4). Extracted REY concentrations are influenced not only by the exchangeable cations (NH_4^+, Na^+, etc) but also by the reagents (sulfate, acetate, chloride, etc). It is difficult to compare the ion-exchange efficiency of ammonium sulfate and sodium acetate. Moldoveanu and Papangelakis (2012) also indicated that more REY are extracted from the ores with decreasing pH of solutions. In the present study, the difference in extracted REY concentrations is likely to result from the differences in the reagents and solution pH between sodium acetate solution (pH = 5) and ammonium sulfate solution (pH = 5.7).

The analytical results of all the samples indicate that the majority of REY except Ce is present in the ion-exchangeable fraction (Fig. 2; Table 4). Ion-exchangeable REY excluding Ce range from 136 to 363 ppm (68 - ~100 % relative to whole-rock contents). The significant depletion of ion-exchangeable Ce is recognized in all the samples and it is common in the ion-adsorption type ores (Wu *et al*., 1990; Sanematsu *et al*., 2013). The depletion of Ce can be explained by the precipitation of CeO_2 under oxidized conditions (Fig. 1J and IK) during weathering because the solubility of CeO_2 is lower in oxidized conditions than in reduced conditions in the pH range of soil water (Brookins, 1988). Ce(IV) is present in Mn oxyhydroxide (Fig. 1L), because Ce(III) is commonly adsorbed on Mn oxide and the oxidized Ce(IV) is incorporated in the Mn oxide (Ohta and Kawabe, 2001). Cerium is most abundant in the organic-matter fraction (step 2), and this result implies that CeO_2 was leached by sodium pyrophosphate solution. This fraction has the second highest REY concentrations following the ion-exchangeable fraction (step 1), however Ce accounts for the majority of REY. Cerium is enriched in Fe-Mn-oxides fractions (steps 3 and 4) as well. This Ce enrichment is probably due to the incorporation of Ce into Mn and Fe oxides.

La_N/Yb_N ratios of the ion-exchangeable fraction are significantly higher than those of the other fractions and whole-rock compositions, suggesting that ion-exchangeable REY except Ce are enriched in LREE and depleted in HREE and Y. The depletion of HREE can be recognized in chondrite-normalized REE patterns (Fig. 5), and this mainly results from a difference of weathering resistances between REE fluorocarbonate and zircon. REE fluorocarbonate enriched in LREE was mostly degraded by chemical weathering (Fig. 1H and 1I), in contrast, zircon

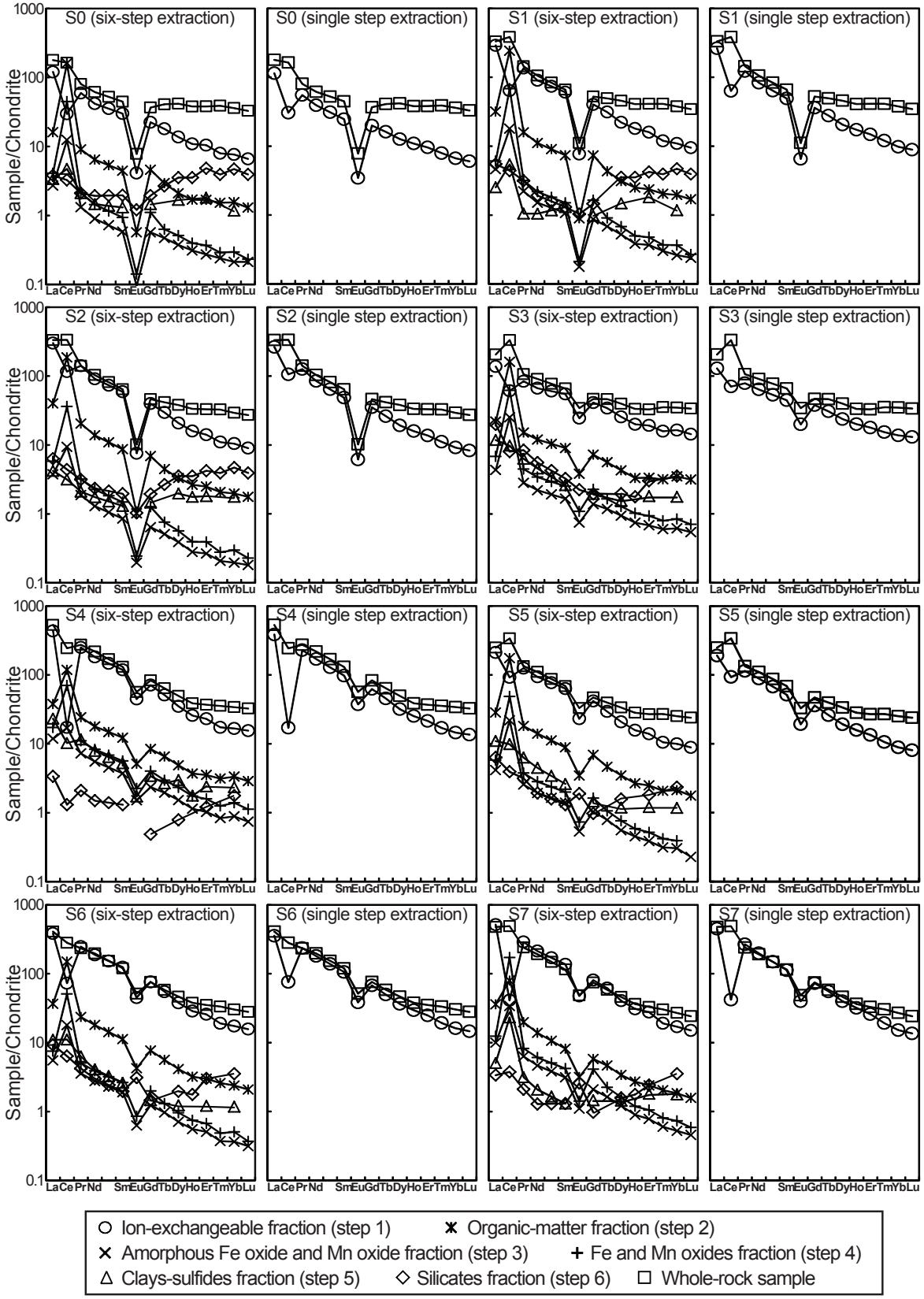

Fig. 5 Chondrite-normalized REE patterns of the each extracted fraction and whole-rock samples in the six-step extraction and single step extraction. The C1-chondrite values are from Sun and McDonough (1989). See Tables 2 and 3 for the experimental conditions.

did not undergo chemical weathering significantly (Fig. 1A, 1B, 1C and 1F). The enrichment of HREE can be seen in the silicates-fraction (step 6), represented by low La_N/Yb_N ratios of 1.0 – 5.6 and chondrite-normalized REE patterns (Fig. 5). This is likely to result from zircon partly leached by the mixture acid. Since zircon was not totally degraded by the acid, large amounts of HREE are present in the estimated residual fraction (Table 4). Huang *et al*. (1989) indicated that typical HREE-rich ion-adsorption ores in Longnan were derived from fractionated granite abundant in synchysite-(Y), which is HREE-rich fluorocarbonate. The ion-exchangeable fraction of these ores would be enriched in HREE because synchysite-(Y) was soluble in soil water and HREE were adsorbed on clays. Sanematsu *et al*. (2013) indicated that LREE-rich ion-adsorption ores in Phuket of Thailand were formed by the parent granite containing abundant fluorocarbonate which is enriched in LREE. These results suggest that the fractionation between LREE and HREE in ion-adsorption ores is constrained by LREE or HREE abundances in primary REE-bearing minerals and their resistances to chemical weathering.

Whole-rock contents of Eu and ion-exchangeable Eu concentrations are low in all the samples. This is consistent with typical ion-adsorption ores depleted in Eu (Wu *et al*., 1990; Bao and Zhao, 2008). A significant amount of Eu was extracted from the mixture acid fraction (step 6) as well (Table 4), and this suggests that residual plagioclase, the dominant Eu-bearing mineral, was leached by the acid.

Scandium can be included in one of rare earth elements in a broad sense, however the ion-exchangeable Sc concentrations are estimated to be low (up to 0.3 ppm Sc; Appendix). In general, Sc is incorporated in pyroxene and amphibole of ultramafic or mafic rocks, and granite is not enriched in Sc (Sanematsu *et al*., 2012). These results suggest that ion-adsorption ores rarely have a potential to recover Sc with REY in terms of amount of resource.

These geochemical features of the ion-adsorption ores are not significantly different from the three weathered granite samples collected outside from a mining site. The grades of the studied ion-adsorption ores are lower than the typical ores of South China, reported by Wu *et al*. (1990) and Bao and Zhao (2008).

5.2 Th and U in ion-adsorption ores

Thorium was ion-exchanged by sodium acetate solution (3.7 – 9.4 % of whole-rock content), but was rarely ion-exchanged by ammonium sulfate solution (<1 % of whole-rock content) as shown in Figure 3. This significant difference in the concentrations is presumably due to the different ligands of acetate and sulfate ligands rather than to different pH. Thorium is predominantly present by complexing with organic and inorganic ligands in solution at a room temperature (Langmuir and Herman, 1980). Thorium(IV) is complexed with acetate at a wide range of pH (Portanova et al., 1975; Rao *et al*., 2004). In contrast, Th-sulfate complex is insignificant at pH > ~5.5 (Langmuir and Herman, 1980), and this caused low Th concentrations extracted by ammonium sulfate solution of pH=5.7.

Thorium is dominantly present in the organic-matter fraction, and is moderately contained in the clays-sulfides fraction and estimated residual fraction (Fig. 3). The residual fraction may suggest the occurrence of insoluble Th silicates (thorite and/ore huttonite). The host materials of Th are not well understood in the organic-matter fraction and clays-sulfides fraction.

Uranium was ion-exchanged by both sodium acetate and ammonium sulfate solutions and the extracted concentrations are lower in the ammonium sulfate solution. This difference results from the differences in reagents and pH. Uranium(VI) is likely to exist as uranyl (UO_2^{2-}) ion, uranyl-acetate complex or uranyl-sulfate complex in the extracted solutions, because these ion and complexes are common as well as other organic and inorganic complexes at room temperature (Langmuir, 1978; Nguyen-Trung *et al*., 1992). Since the stability constants of uranyl-acetate and sulfate complexes are not significantly different (Nguyen-Trung *et al*., 1992), the difference in pH (5.0 and 5.7) may have more influenced the extracted REY concentrations.

Uranium is extensively present in the estimated residual fraction, silicates fraction, ion-exchangeable fraction, clays-sulfides fraction, and organic-matter fraction, however it is rarely present in the Fe-Mn-oxides fractions (Fig. 4). Uranium in the residual and silicates fractions may be derived from zircon and other minerals. Fergusonite ($YNbO_4$), uraninite (UO_2) and coffinite[$(U,Th)SiO_4 \cdot nH_2O$] are relatively common U-bearing minerals in granites, however they were not found on the polished mounts by SEM-EDS. The host materials of U are not well understood in the clays-sulfides fraction and organic-matter fraction.

6. Conclusions

Extraction experiments were conducted on the five ion-adsorption ore samples from South China. The concentrations of ion-exchangeable elements by 1 M sodium acetate solution (pH = 5) range from 174 to 388 ppm REY (43 – 68 % relative to whole-rock contents), from 1.1 to 3.5 ppm Th (3.7 – 9.4 %) and from 0.44 to 1.0 ppm U (14 – 25 %). The concentrations of the ion-exchangeable elements by ammonium sulfate solution (pH = 5.7) range from 170 to 346 ppm REY (42 – 64 %), from 0.03 to 0.31 ppm Th (0.1 – 0.8 %) and from 0.25 to 0.71 ppm U (8 – 18 %).

The ion-exchangeable fraction is significantly depleted in

Ce because Ce was immobilized as Ce(IV) during weathering before the other REE(III) and Y were adsorbed on weathering products in the ores.

The ion-exchangeable fraction is slightly depleted in HREE and Y relative to whole-rock compositions. The fractionation between LREE and HREE is most likely to be constrained by weathering resistances of primary REE-bearing minerals in the studied samples.

Non-ion-exchangeable REY in the ores are present in residual minerals such as fluorocarbonates-(Ce), monazite-(Ce), REE phosphate-silicate (probably britholite-(Ce)), cerianite and zircon. HREE and Y are dominantly contained in zircon.

The majority of Th and U in the ores are present in organic matter, acid-leachable minerals (e.g., clays, sulfides, silicates) and insoluble minerals. The extracted Th and U concentrations are influenced by the reagents and solution pH.

Acknowledgements: We are grateful to Dr. Katsuhiro Tsukimura for reviewing our manuscript and giving helpful comments. Part of this study was supported by the Grant-in-Aid for Young Scientists (B) of No. 23760796 provided by Japan Society for Promotion of Science (JSPS) and by JSPS Postdoctoral Fellowships for Research Abroad.

References

Bao, Z. and Zhao, Z. (2008) Geochemistry of mineralization with exchangeable REY in the weathering crusts of granitic rocks in South China. *Ore Geol. Rev.*, **33**, 519–535.

Brookins, D. G. (1988) *Eh-pH Diagrams for Geochemistry*, Springer, Berlin, 176p.

Chi, R. and Tian, J. (2009) *Weathered Crust Elution-Deposited Rare Earth Ores*, Nova Science Publishers, New York, 288p.

Guo, C. L., Chen, Y. C., Zeng, Z. L. and Lou, F. S. (2012) Petrogenesis of the Xihuashan granites in southeastern China: Constraints from geochemistry and in-situ analyses of zircon U-Pb-Hf-O isotopes. *Lithos*, **148**, 209-227.

Huang, D. H., Wu, C. G. and Han, J. Z. (1989) REE geochemistry and mineralization characteristics of the Zudong and Guanxi Granites, Jiangxi Province. *Acta Geol. Sinica*, **2**, 139-157.

Imai, A., Yonezu, K., Sanematsu, K., Ikuno, T., Ishida, S., Watanabe, K., Pisutha-Arnond, V., Nakapadungrat, S. and Boosayasak, J. (2013) Rare earth elements in hydrothermally altered granitic rocks in the Ranong and Takua Pa tin-field, southern Thailand. *Resource Geol.*, **63**, 84–98.

Ishihara, S., Renmin, H., Hoshino, M. and Murakami, H. (2008) REE abundance and REE minerals in granitic rocks in the Nanling Range, Jiangxi Province, Southern China, and generation of the REE-rich weathered crust deposits. *Resource Geol.*, **58**, 355–372.

Langmuir, D. (1978) Uranium solution – Mineral equilibria at low temperatures with applications to sedimentary ore deposits. *Geochim. Cosmochim. Acta*, **42**, 547-569.

Langmuir, D. and Herman, J. S. (1980) The mobility of thorium in natural waters at low temperatures. *Geochim. Cosmochim. Acta*, **44**, 1753-1766.

Le Couteur, P. C. (2011) *Geological Report on the Chambe Basin Area of Exclusive Prospecting License EPL0325/11 Mulanje Massif, Southern Malawi, East Africa.* 101p.

Moldoveanu, G. A. and Papangelakis, V. G. (2012) Recovery of rare earth elements adsorbed on clay minerals: I. Desorption mechanism. *Hydrometallurgy*, **117-118**, 71-78.

Moldoveanu, G. A. and Papangelakis, V. G. (2013a) Recovery of rare earth elements adsorbed on clay minerals: II. Leaching with ammonium sulfate. *Hydrometallurgy*, **131-132**, 158-156.

Moldoveanu, G. A. and Papangelakis, V. G. (2013b) *Leaching of Rare Earths Elements from Clay Materials – Summary Report to Tantalus Rare Earths AG January 9, 2013.* Department of Chemical Engineering and Applied Chemistry, University of Toronto, 1-9.

Murakami, H. and Ishihara, S. (2008) REE mineralization of weathered crust and clay sediment on granitic rocks in the Sanyo Belt, SW Japan and the southern Jiangxi Province, China. *Resource Geol.*, **58**, 373-401.

Nguyen-Trung, C., Begun, G. M. and Palmer, D. A. (1992) Aqueous uranium complexes. 2. Raman spectroscopic study of the complex formation of the dioxouranium(VI) ion with a variety of inorganic and organic ligands. *Inorg. Chem.*, **31**, 5280-5287.

Ohta, A. and Kawabe, I. (2001) REE(III) adsorption onto Mn dioxide (δ-MnO_2) and Fe oxyhydroxide: Ce(III) oxidation by δ-MnO_2. *Geochim. Cosmochim. Acta*, **65**, 695–703.

Portanova, R., Bernardo, P. Di, Traverso, O., Mazzocchin, G. A. and Magon, L. (1975) Thermodynamic properties of actinide complexes-II. *J. Inorg. Nucl. Chem.*, **37**, 2177-2179.

Rao, L., Zhang, Z., Zanonato, P. L., Bernardo, P. D., Bismondo, A. and Clark, S. B. (2004) Complexation of thorium(IV) with acetate at variable temperatures. *Dalton Trans.*, **18**, 2867-2872.

Roskill (2011) *Rare Earths & Yttrium: Market Outlook to 2015, 14th edition, 2011*, Roskill Information Services, Ltd., London, 492p.

Sanematsu, K., Murakami, H., Watanabe, Y., Duangsurigna, S. and Vilayhack, S. (2009) Enrichment of rare earth elements (REE) in granitic rocks and their weathered crusts in central

and southern Laos. *Bull. Geol. Surv. Japan*, **60**, 527–558.

Sanematsu, K., Hoshino, M. and Watanabe, Y. (2012) Lateritic scandium-bearing deposits. *Shigen Chishitsu*, **62**, 17-26 (in Japanese with English abstract).

Sanematsu, K., Kon, Y., Imai, A., Watanabe, K. and Watanabe, Y. (2013) Geochemical and mineralogical characteristics of ion-adsorption type REE mineralization in Phuket, Thailand. *Mineral. Deposita*, **48**, 437-451.

Sun, S. S. and McDonough, W. F. (1989) Chemical and isotopic systematics of oceanic basalts: implications for mantle composition and processes. *In* Saunders, A.D. and Norry, M.J., eds., *Magmatism in the Ocean Basins, Geological Society Special Publication*, no. 42, 313-345.

Wang, F. Y., Ling, M. X., Ding, X., Hu, Y. H., Zhou, J. B., Yang, X. Y., Liang, H. Y., Fan, W. M. and Sun, S. W. (2011) Mesozoic large magmatism events and mineralization in SE China: oblique subduction of the Pacific plate. *Intern. Geol. Rev.*, **53**, 704-726.

Wu, C. G., Huang, D. H. and Guo, Z. G. (1990) REE geochemistry in the weathered crust of granites, Longnan area, Jiangxi Province. *Acta Geol. Sinica*, **3**, 193-210.

Wu, C. G., Bai, G. and Huang, D. H. (1992) Characteristics and significance of HREE-rich granitoids of the Nanling Mountain area. *Bull. Chinese Acad. Geol. Sci.,* **25**, 43-58 (in Chinese with English abstract).

Zhang, F. F., Wang, Y. J., Zhang, A. M., Fan, W. M., Zhang, Y. Z. and Zi, J. (2012) Geochronological and geochemical constraints on the petrogenesis of Middle Paleozoic (Kwangsian) massive granites in the eastern South China Block. *Lithos*, **150**, 188-208.

Zhou, X. M., Sun, T., Shen, W. Z., Shu, L. S. and Niu, Y. L. (2006) Petrogenesis of Mesozoic granitoids and volcanic rocks in South China: a response to tectonic evolution. *Episodes*, **29**, 26–33.

Recieved August 13, 2013
Accepted December 17, 2013

Appendix Concentrations of extracted elements in the six-step and single step extraction experiments.

	Fraction	Li ppm	Na ppm	Mg ppm	Al ppm	Si ppm	P ppm	K ppm	Ca ppm	Sc ppm	Ti ppm	V ppm	Cr ppm	Mn ppm
S0	Ion-exchangeable (sodium acetate)	<0.1	n.a.	n.a.	n.a.	n.a.	n.a.	n.a.	n.a.	<0.2	<0.4	<0.02	<0.1	22
	Organic matter	1	n.a.	n.a.	n.a.	n.a.	n.a.	n.a.	n.a.	2.3	n.a.	1.6	<0.5	106
	Amorphous Fe oxide and Mn oxide	0.11	n.a.	n.a.	n.a.	n.a.	n.a.	n.a.	n.a.	<0.2	0.6	<0.5	<5	34
	Fe and Mn oxides	0.16	n.a.	n.a.	n.a.	n.a.	n.a.	n.a.	n.a.	<0.2	<0.5	<0.5	<5	4
	Clays and sulfides	1.5	20	20	840	n.a.	n.a.	20	n.a.	0.3	n.a.	3	3	13
	Silicates	6.4	310	80	2680	n.a.	n.a.	1330	n.a.	n.a.	n.a.	3	4.1	14
	Whole-rock content	n.a.	1039	1210	75700	361000	87	34700	140	n.a.	1500	15	< 20	85
	Ion-exchangeable (ammonium sulfate)	n.a.	12	22	69	226	<18	318	8	<0.05	<1.5	<0.2	<0.2	26
S1	Ion-exchangeable (sodium acetate)	<0.1	n.a.	n.a.	n.a.	n.a.	n.a.	n.a.	n.a.	<0.2	<0.4	<0.02	<0.1	17
	Organic matter	<1	n.a.	n.a.	n.a.	n.a.	n.a.	n.a.	n.a.	2.2	n.a.	1.8	<0.5	48
	Amorphous Fe oxide and Mn oxide	0.07	n.a.	n.a.	n.a.	n.a.	n.a.	n.a.	n.a.	<0.2	0.5	<0.5	<5	14
	Fe and Mn oxides	0.07	n.a.	n.a.	n.a.	n.a.	n.a.	n.a.	n.a.	<0.2	<0.5	<0.5	<5	2
	Clays and sulfides	1.4	10	10	700	n.a.	n.a.	20	n.a.	0.2	n.a.	3	1	6
	Silicates	8.1	400	90	2680	n.a.	n.a.	1370	n.a.	n.a.	n.a.	6	4.2	8
	Whole-rock content	n.a.	1039	1330	76400	364000	87	31500	140	n.a.	1380	13	< 20	116
	Ion-exchangeable (ammonium sulfate)	n.a.	15	22	76	252	<18	325	5	<0.05	<1.5	<0.2	<0.2	20
S2	Ion-exchangeable (sodium acetate)	<0.1	n.a.	n.a.	n.a.	n.a.	n.a.	n.a.	n.a.	<0.2	<0.4	<0.02	<0.1	29
	Organic matter	1	n.a.	n.a.	n.a.	n.a.	n.a.	n.a.	n.a.	2.5	n.a.	2	0.7	56
	Amorphous Fe oxide and Mn oxide	<0.05	n.a.	n.a.	n.a.	n.a.	n.a.	n.a.	n.a.	<0.2	<0.5	<0.5	<5	20
	Fe and Mn oxides	0.12	n.a.	n.a.	n.a.	n.a.	n.a.	n.a.	n.a.	<0.2	<0.5	<0.5	<5	2
	Clays and sulfides	1.6	10	10	660	n.a.	n.a.	20	n.a.	0.2	n.a.	<1	0.7	8
	Silicates	8.1	410	100	2660	n.a.	n.a.	1070	n.a.	n.a.	n.a.	3	4.4	11
	Whole-rock content	n.a.	890	1390	79400	356000	87	29800	210	n.a.	1380	14	< 20	93
	Ion-exchangeable (ammonium sulfate)	n.a.	16	19	92	237	<18	260	4	<0.05	<1.5	<0.2	<0.2	36
S3	Ion-exchangeable (sodium acetate)	0.5	n.a.	n.a.	n.a.	n.a.	n.a.	n.a.	n.a.	0.3	<0.4	<0.02	<0.1	105
	Organic matter	3	n.a.	n.a.	n.a.	n.a.	n.a.	n.a.	n.a.	2.9	n.a.	2.5	0.8	205
	Amorphous Fe oxide and Mn oxide	0.22	n.a.	n.a.	n.a.	n.a.	n.a.	n.a.	n.a.	<0.2	1.2	<0.5	<5	84
	Fe and Mn oxides	0.42	n.a.	n.a.	n.a.	n.a.	n.a.	n.a.	n.a.	<0.2	1.1	<0.5	<5	13
	Clays and sulfides	5	10	20	1010	n.a.	n.a.	20	n.a.	1.5	n.a.	5	2.9	27
	Silicates	14.3	410	110	2740	n.a.	n.a.	670	n.a.	n.a.	n.a.	4	4.6	34
	Whole-rock content	n.a.	742	1450	89000	326000	87	24200	140	n.a.	2640	16	< 20	503
	Ion-exchangeable (ammonium sulfate)	n.a.	10	23	85	220	<18	203	2	0.11	<1.5	<0.2	<0.2	157
S4	Ion-exchangeable (sodium acetate)	0.3	n.a.	n.a.	n.a.	n.a.	n.a.	n.a.	n.a.	<0.2	<0.4	<0.02	<0.1	34
	Organic matter	4	n.a.	n.a.	n.a.	n.a.	n.a.	n.a.	n.a.	2.4	n.a.	1.7	1.2	136
	Amorphous Fe oxide and Mn oxide	0.37	n.a.	n.a.	n.a.	n.a.	n.a.	n.a.	n.a.	<0.2	1.6	<0.5	<5	69
	Fe and Mn oxides	0.67	n.a.	n.a.	n.a.	n.a.	n.a.	n.a.	n.a.	<0.2	1	<0.5	<5	10
	Clays and sulfides	9.2	10	40	1180	n.a.	n.a.	40	n.a.	1.5	n.a.	2	1.7	42
	Silicates	13.2	240	30	1280	n.a.	n.a.	1640	n.a.	n.a.	n.a.	6	5.3	25
	Whole-rock content	n.a.	1040	1630	75900	345000	131	34400	140	n.a.	2460	10	< 20	395
	Ion-exchangeable (ammonium sulfate)	n.a.	13	28	47	254	<18	288	2	<0.05	<1.5	<0.2	<0.2	39
S5	Ion-exchangeable (sodium acetate)	0.8	n.a.	n.a.	n.a.	n.a.	n.a.	n.a.	n.a.	0.3	<0.4	<0.02	<0.1	35
	Organic matter	3	n.a.	n.a.	n.a.	n.a.	n.a.	n.a.	n.a.	3.5	n.a.	3.2	0.7	70
	Amorphous Fe oxide and Mn oxide	0.2	n.a.	n.a.	n.a.	n.a.	n.a.	n.a.	n.a.	<0.2	0.7	<0.5	<5	26
	Fe and Mn oxides	0.39	n.a.	n.a.	n.a.	n.a.	n.a.	n.a.	n.a.	<0.2	<0.5	<0.5	<5	9
	Clays and sulfides	3.7	10	40	810	n.a.	n.a.	30	n.a.	0.9	n.a.	3	2.2	26
	Silicates	9.1	420	60	2180	n.a.	n.a.	1390	n.a.	n.a.	n.a.	4	3.4	12
	Whole-rock content	n.a.	1630	1870	85400	329000	87	32800	140	n.a.	2340	17	< 20	240
	Ion-exchangeable (ammonium sulfate)	n.a.	13	47	180	248	<18	366	3	0.13	<1.5	<0.2	<0.2	44
S6	Ion-exchangeable (sodium acetate)	0.1	n.a.	n.a.	n.a.	n.a.	n.a.	n.a.	n.a.	<0.2	<0.4	<0.02	<0.1	33
	Organic matter	2	n.a.	n.a.	n.a.	n.a.	n.a.	n.a.	n.a.	2.7	n.a.	2.4	0.5	72
	Amorphous Fe oxide and Mn oxide	0.15	n.a.	n.a.	n.a.	n.a.	n.a.	n.a.	n.a.	<0.2	1.1	<0.5	<5	20
	Fe and Mn oxides	0.32	n.a.	n.a.	n.a.	n.a.	n.a.	n.a.	n.a.	<0.2	<0.5	<0.5	<5	6
	Clays and sulfides	4.7	20	40	820	n.a.	n.a.	50	n.a.	1.3	n.a.	3	2	32
	Silicates	9.6	340	110	3350	n.a.	n.a.	1200	n.a.	n.a.	n.a.	3	5	22
	Whole-rock content	n.a.	1930	1390	89700	333000	87	37100	210	n.a.	2340	14	< 20	209
	Ion-exchangeable (ammonium sulfate)	n.a.	15	35	120	207	<18	350	3	0.09	<1.5	<0.2	<0.2	49
S7	Ion-exchangeable (sodium acetate)	0.2	n.a.	n.a.	n.a.	n.a.	n.a.	n.a.	n.a.	<0.2	<0.4	<0.02	<0.1	34
	Organic matter	2	n.a.	n.a.	n.a.	n.a.	n.a.	n.a.	n.a.	1.7	n.a.	1	<0.5	117
	Amorphous Fe oxide and Mn oxide	0.44	n.a.	n.a.	n.a.	n.a.	n.a.	n.a.	n.a.	<0.2	1.1	<0.5	<5	108
	Fe and Mn oxides	0.72	n.a.	n.a.	n.a.	n.a.	n.a.	n.a.	n.a.	<0.2	0.6	<0.5	<5	19
	Clays and sulfides	7.2	10	60	1070	n.a.	n.a.	70	n.a.	1.5	n.a.	5	3.1	47
	Silicates	8.7	320	80	3510	n.a.	n.a.	1410	n.a.	n.a.	n.a.	2	6.8	27
	Whole-rock content	n.a.	2230	1690	75200	353000	87	42300	140	n.a.	2160	9	< 20	441
	Ion-exchangeable (ammonium sulfate)	n.a.	18	41	113	174	<18	392	5	<0.05	<1.5	<0.2	<0.2	47

See Tables 2 and 3 for the experiment conditions.
Whole-rock content data are from Murakami and Ishihara (2008).
n.a., not analyzed.

Appendix (continued)

	Fraction	Fe ppm	Co ppm	Ni ppm	Cu ppm	Zn ppm	Ga ppm	Ge ppm	As ppm	Rb ppm	Sr ppm	Y ppm	Zr ppm	Nb ppm
S0	Ion-exchangeable (sodium acetate)	n.a.	0.53	<0.03	<0.1	<2	0.51	0.05	0.13	2.7	0.3	20.3	<0.08	<0.001
	Organic matter	n.a.	3.0	<1	<0.6	18	2.8	<0.3	0.5	27	0.2	2.8	1.2	0.25
	Amorphous Fe oxide and Mn oxide	n.a.	0.73	<0.08	<0.04	<0.5	0.23	<0.01	<0.04	1.0	<0.1	0.49	<0.4	0.006
	Fe and Mn oxides	n.a.	0.08	<0.08	<0.04	0.8	0.23	<0.01	<0.04	1.2	<0.1	0.16	<0.4	0.012
	Clays and sulfides	380	0.5	0.5	0.41	10.9	3.4	<0.1	5.1	14	1.7	2.0	0.9	0.2
	Silicates	190	0.5	0.6	<0.2	7.2	9.9	0.1	79	74	32.4	4.3	60	23.7
	Whole-rock content	15700	57	< 20	< 10	50	25	1.8	<5	291	12	64.9	179	51.8
	Ion-exchangeable (ammonium sulfate)	<6	0.24	<0.2	<0.4	0.43	2.3	n.a.	0.40	5.3	0.23	18.4	<0.5	<0.004
S1	Ion-exchangeable (sodium acetate)	n.a.	0.33	<0.03	<0.1	<2	0.46	0.12	0.25	2.5	0.2	30.4	<0.08	<0.001
	Organic matter	n.a.	1.5	<1	<0.6	13	2.6	<0.3	0.60	24	0.1	4.0	1.3	0.24
	Amorphous Fe oxide and Mn oxide	n.a.	0.30	<0.08	<0.04	<0.5	0.22	<0.01	<0.04	0.9	<0.1	0.61	<0.4	0.006
	Fe and Mn oxides	n.a.	0.05	<0.08	<0.04	<0.5	0.25	<0.01	<0.04	1.1	<0.1	0.17	<0.4	0.013
	Clays and sulfides	260	0.3	0.4	0.29	6.9	2.4	<0.1	2.5	10	1.2	1.65	0.7	0.2
	Silicates	140	0.5	0.7	<0.2	6.2	9.3	0.1	75	76	36.3	5.30	63	19.7
	Whole-rock content	14100	60	< 20	< 10	30	25	1.5	<5	253	12	71.2	172	49.2
	Ion-exchangeable (ammonium sulfate)	<6	0.12	<0.2	<0.4	<0.3	2.2	n.a.	0.88	5.6	0.17	28.7	<0.5	<0.004
S2	Ion-exchangeable (sodium acetate)	n.a.	0.86	0.04	<0.1	3	1.3	0.12	0.23	2.9	0.2	26.7	<0.08	<0.001
	Organic matter	n.a.	3.0	<1	<0.6	19	3.0	<0.3	0.7	22	0.1	4.4	1.7	0.23
	Amorphous Fe oxide and Mn oxide	n.a.	0.39	<0.08	<0.04	<0.5	0.13	<0.01	<0.04	0.8	<0.1	0.43	<0.4	0.002
	Fe and Mn oxides	n.a.	0.10	<0.08	<0.04	<0.5	0.18	<0.01	<0.04	0.9	<0.1	0.22	<0.4	0.010
	Clays and sulfides	380	0.6	0.5	0.22	9.8	2.4	<0.1	1.8	8.5	0.9	2.4	0.7	0.1
	Silicates	230	1.1	0.9	<0.2	8.7	8.5	<0.1	79	54	31.1	5.1	51	16.2
	Whole-rock content	16000	53	140	70	50	25	2	<5	239	12	59.5	143	37.1
	Ion-exchangeable (ammonium sulfate)	<6	0.56	<0.2	0.8	0.71	2.3	n.a.	0.92	5.7	0.19	26.0	<0.5	<0.004
S3	Ion-exchangeable (sodium acetate)	n.a.	0.47	<0.03	<0.1	<2	0.16	0.09	0.16	3.4	0.2	30.5	<0.08	<0.001
	Organic matter	n.a.	2.8	<1	0.7	16	3.2	<0.3	0.9	26	0.2	4.3	2.2	0.43
	Amorphous Fe oxide and Mn oxide	n.a.	1.1	<0.08	0.06	<0.5	0.32	<0.01	<0.04	1.0	<0.1	0.86	<0.4	0.009
	Fe and Mn oxides	n.a.	0.09	<0.08	0.06	0.8	0.31	<0.01	<0.04	1.7	<0.1	0.35	<0.4	0.016
	Clays and sulfides	840	0.5	0.7	0.55	19.1	4.7	<0.1	3.2	18	1.6	1.7	2.2	0.3
	Silicates	260	0.3	0.8	<0.2	10.4	8.6	<0.1	67	34	40.1	2.7	41	1.2
	Whole-rock content	31300	56	< 20	< 10	70	29	2.4	<5	189	24	49.8	474	43.9
	Ion-exchangeable (ammonium sulfate)	<6	0.55	<0.2	<0.4	0.43	0.81	n.a.	0.69	5.1	0.15	28.5	<0.5	<0.004
S4	Ion-exchangeable (sodium acetate)	n.a.	0.11	<0.03	<0.1	4	1.2	0.24	0.51	2.2	0.2	38.0	<0.08	<0.001
	Organic matter	n.a.	1.06	<1	<0.6	22	3.5	<0.3	0.5	12	0.2	4.8	1.1	0.21
	Amorphous Fe oxide and Mn oxide	n.a.	0.47	<0.08	0.06	1.3	0.47	0.02	<0.04	1.0	<0.1	1.5	<0.4	0.003
	Fe and Mn oxides	n.a.	0.05	<0.08	0.07	1.7	0.42	<0.01	<0.04	1.2	<0.1	0.70	<0.4	0.007
	Clays and sulfides	1160	0.6	0.6	0.34	27	5.72	<0.1	2.8	12	1.4	2.3	2	<0.1
	Silicates	380	0.3	0.7	<0.2	13.8	12	0.1	78	40	28.2	0.7	39	21.6
	Whole-rock content	29200	52	< 20	< 10	50	24	1.9	<5	183	27	56.6	400	39.9
	Ion-exchangeable (ammonium sulfate)	<6	<0.05	<0.2	<0.4	0.57	2.0	n.a.	1.9	3.6	0.20	35.6	<0.5	<0.004
S5	Ion-exchangeable (sodium acetate)	n.a.	2.5	0.1	0.1	3	0.44	0.14	0.26	3.5	0.2	24.6	<0.08	<0.001
	Organic matter	n.a.	6.7	<1	1.3	27	3.5	<0.3	1.1	20	0.3	3.9	4.4	0.34
	Amorphous Fe oxide and Mn oxide	n.a.	1.4	<0.08	0.08	<0.5	0.27	<0.01	<0.04	1.3	<0.1	0.56	<0.4	0.004
	Fe and Mn oxides	n.a.	0.23	<0.08	0.11	1.1	0.22	<0.01	<0.04	1.2	<0.1	0.19	<0.4	0.010
	Clays and sulfides	810	1.0	0.6	1.1	24.9	3.5	<0.1	3.2	10	1.3	1.05	2.2	0.1
	Silicates	160	0.4	<0.5	<0.2	6.4	8.4	<0.1	63.7	40	36.6	1.9	40	2.9
	Whole-rock content	29200	59	< 20	< 10	50	27	1.5	<5	213	32	46	358	35.3
	Ion-exchangeable (ammonium sulfate)	<6	1.61	<0.2	<0.4	0.78	2.2	n.a.	0.9	8.0	0.19	23.5	<0.5	<0.004
S6	Ion-exchangeable (sodium acetate)	n.a.	0.80	0.04	<0.1	2	0.81	0.26	0.55	3.5	0.3	43.4	<0.08	<0.001
	Organic matter	n.a.	3.8	<1	1	22	2.9	<0.3	0.9	19	0.3	4.9	3.3	0.34
	Amorphous Fe oxide and Mn oxide	n.a.	1.3	<0.08	0.04	<0.5	0.26	<0.01	<0.04	1.2	<0.1	0.74	<0.4	0.004
	Fe and Mn oxides	n.a.	0.13	<0.08	0.24	1.2	0.24	<0.01	<0.04	1.3	<0.1	0.25	<0.4	0.012
	Clays and sulfides	980	0.8	0.8	1.2	26.6	3.9	<0.1	3.4	14	1.9	1.36	2.2	0.1
	Silicates	240	0.3	<0.5	<0.2	9.8	13.8	0.2	74	54	46.4	2.8	51	7.3
	Whole-rock content	25700	61	< 20	< 10	60	25	1.8	<5	228	37	62	384	35.2
	Ion-exchangeable (ammonium sulfate)	<6	0.77	<0.2	<0.4	0.58	3.6	n.a.	2.0	6.9	0.21	35.1	<0.5	<0.004
S7	Ion-exchangeable (sodium acetate)	n.a.	0.42	<0.03	<0.1	4	1.5	0.30	0.66	2.8	0.5	51	<0.08	0.006
	Organic matter	n.a.	2.4	<1	<0.6	17	2.3	<0.3	0.4	11	0.3	4.3	1.5	0.26
	Amorphous Fe oxide and Mn oxide	n.a.	2.2	<0.08	0.09	1.8	0.41	0.01	<0.04	1.4	<0.1	1.3	<0.4	0.003
	Fe and Mn oxides	n.a.	0.32	0.08	0.13	3.4	0.51	<0.01	<0.04	1.4	<0.1	0.32	<0.4	0.013
	Clays and sulfides	1200	0.9	0.9	1.2	40.5	5.6	<0.1	4.8	19	1.5	1.6	2.9	0.1
	Silicates	350	0.3	<0.5	<0.2	11.4	16.8	0.2	73	49	41.7	2	52	10.1
	Whole-rock content	22900	79	< 20	< 10	80	24	2.1	<5	239	44	62.3	375	35.4
	Ion-exchangeable (ammonium sulfate)	<6	0.22	<0.2	<0.4	0.72	2.8	n.a.	2.2	4.7	0.47	39.5	<0.5	<0.004

See Tables 2 and 3 for the experiment conditions.
Whole-rock content data are from Murakami and Ishihara (2008).
n.a., not analyzed.

Appendix (continued)

	Fraction	Mo ppm	Sn ppm	Sb ppm	Cs ppm	Ba ppm	La ppm	Ce ppm	Pr ppm	Nd ppm	Sm ppm	Eu ppm	Gd ppm	Tb ppm
S0	Ion-exchangeable (sodium acetate)	<0.02	<0.01	<0.005	0.035	15	28.5	18.2	5.66	19.5	4.59	0.24	4.60	0.67
	Organic matter	0.38	n.a.	<0.02	0.84	5.5	3.82	98.1	0.86	3.01	0.68	0.033	0.94	0.11
	Amorphous Fe oxide and Mn oxide	<0.02	<0.1	<0.005	0.06	1.4	0.64	7.6	0.13	0.42	0.089	0.006	0.12	0.018
	Fe and Mn oxides	<0.02	<0.1	<0.005	0.08	<0.05	0.33	19.8	0.08	0.25	0.054	0.003	0.11	0.006
	Clays and sulfides	0.33	0.34	0.05	0.33	2.8	0.8	2.9	0.2	0.68	0.2	<0.1	0.3	<0.1
	Silicates	0.2	4	3.6	1.3	78	0.9	2	0.2	0.9	0.3	0.07	0.4	0.1
	Whole-rock content	< 2	4	3	4.8	93	42.4	100	7.62	28.7	6.83	0.453	7.54	1.53
	Ion-exchangeable (ammonium sulfate)	<0.4	n.a.	n.a.	0.31	11	27.1	18.7	5.24	18.3	3.76	0.20	4.09	0.60
S1	Ion-exchangeable (sodium acetate)	<0.02	<0.01	<0.005	0.041	13	68.8	39.1	12.9	42.1	9.25	0.446	8.29	1.17
	Organic matter	0.46	n.a.	<0.02	1.6	4.5	7.5	148	1.5	5.2	1.1	0.052	1.5	0.16
	Amorphous Fe oxide and Mn oxide	<0.02	<0.1	<0.005	0.07	1.13	1.1	11	0.21	0.71	0.16	0.010	0.18	0.026
	Fe and Mn oxides	<0.02	<0.1	<0.005	0.11	<0.05	0.34	31	0.091	0.31	0.066	0.002	0.16	0.008
	Clays and sulfides	0.37	0.17	0.03	0.7	2.2	0.60	3.3	0.1	0.49	0.2	<0.1	0.2	<0.1
	Silicates	0.2	4	2.7	1.3	73	1.3	2.7	0.3	0.9	0.2	0.06	0.3	<0.1
	Whole-rock content	< 2	4	1	6.3	88	78.6	235	13.7	49.3	10.1	0.645	10.8	1.85
	Ion-exchangeable (ammonium sulfate)	<0.4	n.a.	n.a.	0.43	11	62.4	38.7	11.7	38.9	7.5	0.4	7.4	1.0
S2	Ion-exchangeable (sodium acetate)	<0.02	<0.01	<0.005	0.031	39	71.3	71.3	13.4	42.6	9.06	0.44	8.2	1.11
	Organic matter	0.62	n.a.	<0.02	0.83	10.9	9.5	114	1.9	6.5	1.3	0.059	1.42	0.17
	Amorphous Fe oxide and Mn oxide	<0.02	<0.1	<0.005	0.05	3.1	0.89	5.8	0.18	0.61	0.13	0.011	0.13	0.019
	Fe and Mn oxides	<0.02	<0.1	<0.005	0.08	<0.05	0.49	16.4	0.13	0.45	0.096	0.003	0.13	0.009
	Clays and sulfides	0.49	0.17	0.03	0.26	2.5	1	1.9	0.2	0.82	0.2	<0.1	0.3	<0.1
	Silicates	0.4	3	2.3	1.1	57	1.5	2.7	0.3	1.1	0.3	0.06	0.4	0.1
	Whole-rock content	3	3	3.4	5.0	115	79.0	205	13.4	48.4	9.82	0.591	9.51	1.56
	Ion-exchangeable (ammonium sulfate)	<0.4	n.a.	n.a.	0.35	11	62.7	64.9	12.0	39.6	7.44	0.36	7.24	0.98
S3	Ion-exchangeable (sodium acetate)	<0.02	<0.01	<0.005	0.18	4	32.6	37.5	7.99	31.1	8.41	1.42	8.47	1.28
	Organic matter	0.21	n.a.	<0.02	3.3	6.2	5.2	99	1.4	5.6	1.4	0.22	1.49	0.21
	Amorphous Fe oxide and Mn oxide	<0.02	<0.1	<0.005	0.18	1.01	1.03	15	0.27	1.03	0.26	0.044	0.29	0.044
	Fe and Mn oxides	<0.02	<0.1	<0.005	0.31	<0.05	0.58	23	0.16	0.57	0.13	0.020	0.18	0.018
	Clays and sulfides	0.23	1.25	0.06	1.9	5.3	2.8	6.0	0.6	2.13	0.4	<0.1	0.4	<0.1
	Silicates	<0.1	<0.1	0.2	1.4	160	4.7	4.9	0.8	2.6	0.5	0.13	0.4	<0.1
	Whole-rock content	< 2	4	4.7	11.6	362	48.7	204	10.1	42.4	10.1	1.99	9.58	1.73
	Ion-exchangeable (ammonium sulfate)	<0.4	n.a.	n.a.	0.87	4	30.6	43.2	7.5	29.9	6.82	1.16	7.79	1.15
S4	Ion-exchangeable (sodium acetate)	<0.02	<0.01	<0.005	0.12	36	103.0	10.6	23.8	85.0	18.1	2.59	14.6	1.91
	Organic matter	0.08	n.a.	<0.02	1.9	12.4	8.9	73	2.3	8.3	1.9	0.30	1.7	0.2
	Amorphous Fe oxide and Mn oxide	<0.02	<0.1	<0.005	0.20	4.03	2.8	10	0.69	2.6	0.57	0.088	0.48	0.073
	Fe and Mn oxides	<0.02	<0.1	<0.005	0.24	<0.05	1.3	33	0.36	1.3	0.29	0.043	0.34	0.038
	Clays and sulfides	0.14	1.55	0.05	2.0	14.6	5.5	6.3	1.1	3.68	0.8	0.1	0.7	<0.1
	Silicates	0.2	3	3.7	1.3	321	0.8	0.8	0.2	0.7	0.2	<0.05	0.1	<0.1
	Whole-rock content	< 2	4	2.3	8.3	522	126	149	26.0	102	20.0	3.28	17.1	2.39
	Ion-exchangeable (ammonium sulfate)	<0.4	n.a.	n.a.	0.52	10	91.3	10.4	21.8	79.3	14.9	2.17	12.8	1.70
S5	Ion-exchangeable (sodium acetate)	<0.02	<0.01	<0.005	0.12	12	50.1	56.2	11.9	43.8	9.68	1.34	8.59	1.10
	Organic matter	0.2	n.a.	0.02	2.8	9.6	6.7	107	1.7	6.6	1.4	0.20	1.4	0.17
	Amorphous Fe oxide and Mn oxide	<0.02	<0.1	<0.005	0.20	4.4	0.98	13.4	0.24	0.90	0.21	0.031	0.21	0.029
	Fe and Mn oxides	<0.02	<0.1	<0.005	0.27	<0.05	0.39	16.4	0.11	0.42	0.09	0.012	0.12	0.010
	Clays and sulfides	0.17	0.84	0.78	1.3	4.4	2.6	6.04	0.6	2.09	0.4	<0.1	0.3	<0.1
	Silicates	<0.1	<0.1	0.5	1.4	294	1.5	2.4	0.3	0.9	0.2	0.11	0.2	<0.1
	Whole-rock content	< 2	3	2.2	12.8	550	58.9	207	12.7	51.6	10.5	1.91	9.66	1.48
	Ion-exchangeable (ammonium sulfate)	<0.4	n.a.	n.a.	1.35	11	45.2	57.0	10.8	41.4	7.88	1.12	7.39	0.98
S6	Ion-exchangeable (sodium acetate)	<0.02	<0.01	<0.005	0.12	24	90.7	44.6	23.5	87.7	19.0	2.61	15.6	2.05
	Organic matter	0.17	n.a.	<0.02	2.5	10.7	8.7	92	2.2	8.4	1.7	0.25	1.6	0.21
	Amorphous Fe oxide and Mn oxide	<0.02	<0.1	<0.005	0.17	1.75	1.31	11	0.34	1.3	0.29	0.036	0.25	0.036
	Fe and Mn oxides	<0.02	<0.1	<0.005	0.29	<0.05	0.47	20	0.14	0.53	0.11	0.013	0.16	0.013
	Clays and sulfides	0.21	1.04	0.06	1.4	5.3	2.6	6.8	0.6	1.9	0.40	<0.1	0.30	<0.1
	Silicates	<0.1	<0.1	1.2	1.6	379	2.2	3.9	0.4	1.4	0.3	0.18	0.3	<0.1
	Whole-rock content	< 2	2	2.3	10.2	628	96.8	172	22.2	92	18.3	2.98	15.6	2.18
	Ion-exchangeable (ammonium sulfate)	<0.4	n.a.	n.a.	0.94	18	84.3	46.4	22.4	84.2	16.2	2.2	13.9	1.86
S7	Ion-exchangeable (sodium acetate)	<0.02	<0.01	<0.005	0.07	42	122	25.2	27.4	99.3	20.9	2.76	16.6	2.31
	Organic matter	0.07	n.a.	<0.02	1.1	21.6	8.5	49	1.9	6.5	1.3	0.18	1.2	0.17
	Amorphous Fe oxide and Mn oxide	<0.02	<0.1	<0.005	0.17	17.7	2.4	21	0.60	2.2	0.48	0.064	0.43	0.061
	Fe and Mn oxides	<0.02	<0.1	<0.005	0.23	0.84	0.58	84	0.18	0.67	0.16	0.018	0.41	0.023
	Clays and sulfides	0.28	1.39	0.06	1.6	5.2	1.2	14	0.3	0.97	0.2	<0.1	0.3	<0.1
	Silicates	<0.1	<0.1	1.7	1.5	436	0.8	2.3	0.2	0.6	0.2	0.15	0.2	<0.1
	Whole-rock content	< 2	2	3.8	6.6	774	113	300	22.8	89.5	17.6	2.82	15.3	2.18
	Ion-exchangeable (ammonium sulfate)	<0.4	n.a.	n.a.	0.40	14	106	25.7	25.4	92.6	17.2	2.31	14.9	2.07

See Tables 2 and 3 for the experiment conditions.
Whole-rock content data are from Murakami and Ishihara (2008).
n.a., not analyzed.

Appendix (continued)

	Fraction	Dy ppm	Ho ppm	Er ppm	Tm ppm	Yb ppm	Lu ppm	Hf ppm	Ta ppm	Tl ppm	Pb ppm	Bi ppm	Th ppm	U ppm
S0	Ion-exchangeable (sodium acetate)	3.48	0.62	1.73	0.20	1.30	0.17	0.016	0.003	0.02	14	<0.01	3.3	0.85
	Organic matter	0.53	0.096	0.28	0.039	0.26	0.033	0.052	<0.003	0.20	9	0.08	22.3	0.7
	Amorphous Fe oxide and Mn oxide	0.095	0.018	0.045	0.006	0.036	0.005	<0.005	<0.0005	0.01	2.6	<0.1	0.14	0.05
	Fe and Mn oxides	0.035	0.005	0.016	0.001	0.014	0.001	<0.005	<0.0005	0.01	0.39	<0.1	0.11	0.07
	Clays and sulfides	0.43	<0.1	0.3	<0.1	0.2	<0.1	<0.1	<0.05	0.07	1.5	<0.02	11.5	0.70
	Silicates	0.9	0.2	0.8	0.1	0.8	0.1	2.5	1.8	0.51	7.8	0.08	2.8	1.2
	Whole-rock content	10.6	2.15	6.30	0.993	6.13	0.835	6.4	4.1	1.33	36	0.2	49.9	5.4
	Ion-exchangeable (ammonium sulfate)	3.21	0.62	1.59	0.20	1.13	0.15	n.a.	<0.002	<0.02	6.0	<0.06	0.23	0.55
S1	Ion-exchangeable (sodium acetate)	5.62	1.02	2.64	0.31	1.86	0.24	0.024	0.004	0.02	11	<0.01	3.6	0.94
	Organic matter	0.79	0.14	0.39	0.052	0.33	0.043	0.062	<0.003	0.20	6	<0.04	27.6	0.8
	Amorphous Fe oxide and Mn oxide	0.13	0.022	0.061	0.008	0.045	0.006	<0.005	<0.0005	0.02	1.7	<0.1	0.20	0.05
	Fe and Mn oxides	0.040	0.006	0.018	0.002	0.018	0.001	<0.005	<0.0005	0.02	0.4	<0.1	0.13	0.09
	Clays and sulfides	0.38	<0.1	0.3	<0.1	0.2	<0.1	<0.1	<0.05	0.07	0.99	<0.02	10.8	0.70
	Silicates	0.9	0.2	0.7	0.1	0.8	0.1	2.2	1.2	0.41	5.4	0.06	2.9	1.3
	Whole-rock content	11.6	2.31	6.81	1.05	6.41	0.877	6.3	4.3	0.86	15	<0.1	51.2	5.1
	Ion-exchangeable (ammonium sulfate)	5.2	0.98	2.5	0.3	1.7	0.23	n.a.	<0.002	<0.02	4.8	<0.06	0.17	0.64
S2	Ion-exchangeable (sodium acetate)	5.29	0.904	2.33	0.28	1.78	0.23	0.024	0.004	0.02	32	<0.01	5.4	1.16
	Organic matter	0.84	0.15	0.41	0.053	0.34	0.045	0.067	<0.003	0.20	11	<0.04	23.2	0.8
	Amorphous Fe oxide and Mn oxide	0.099	0.016	0.044	0.005	0.033	0.005	<0.005	<0.0005	0.01	2.5	<0.1	0.16	0.04
	Fe and Mn oxides	0.045	0.006	0.021	0.002	0.017	0.001	<0.005	<0.0005	0.01	0.46	<0.1	0.10	0.06
	Clays and sulfides	0.50	0.1	0.3	<0.1	0.3	<0.1	<0.1	<0.05	0.05	1.5	<0.02	8.8	0.80
	Silicates	0.9	0.2	0.7	0.1	0.8	0.1	2.2	1.1	0.34	5.7	0.08	3.9	1.2
	Whole-rock content	9.68	1.89	5.46	0.834	4.98	0.692	5.2	3.1	0.95	47	0.2	51.3	4.8
	Ion-exchangeable (ammonium sulfate)	4.88	0.90	2.27	0.28	1.56	0.21	n.a.	<0.002	<0.02	13.6	<0.06	0.34	0.83
S3	Ion-exchangeable (sodium acetate)	6.5	1.13	3.18	0.40	2.8	0.37	0.03	0.005	0.07	9.7	<0.01	3.2	0.71
	Organic matter	1.1	0.19	0.56	0.081	0.60	0.08	0.086	0.008	0.40	7	0.09	13.3	0.4
	Amorphous Fe oxide and Mn oxide	0.24	0.042	0.11	0.015	0.11	0.014	<0.005	<0.0005	0.04	4.3	<0.1	0.18	0.03
	Fe and Mn oxides	0.086	0.016	0.042	0.005	0.039	0.004	<0.005	<0.0005	0.03	0.93	<0.1	0.05	0.05
	Clays and sulfides	0.39	<0.1	0.3	<0.1	0.3	<0.1	<0.1	<0.05	0.15	2.9	0.08	6.2	0.80
	Silicates	0.5	0.1	0.5	<0.1	0.6	<0.1	1.4	<0.1	0.22	6	0.09	2.7	1.0
	Whole-rock content	10.1	1.89	5.43	0.902	5.93	0.858	11.9	3.3	1.33	42	0.8	36.8	4.7
	Ion-exchangeable (ammonium sulfate)	6.03	1.14	2.96	0.39	2.34	0.33	n.a.	<0.002	0.07	2.3	<0.06	0.25	0.37
S4	Ion-exchangeable (sodium acetate)	8.88	1.46	3.82	0.44	2.84	0.39	0.034	0.007	0.03	2.32	<0.01	1.1	0.45
	Organic matter	1.2	0.21	0.58	0.08	0.57	0.073	0.051	0.004	0.20	4	<0.04	11.4	0.2
	Amorphous Fe oxide and Mn oxide	0.39	0.065	0.17	0.021	0.15	0.019	<0.005	<0.0005	0.03	2.1	<0.1	0.17	0.04
	Fe and Mn oxides	0.20	0.034	0.093	0.011	0.086	0.010	<0.005	<0.0005	0.03	0.53	<0.1	0.09	0.06
	Clays and sulfides	0.76	0.1	0.4	<0.1	0.4	<0.1	<0.1	<0.05	0.08	4.8	0.06	10.4	0.7
	Silicates	0.2	<0.1	0.2	<0.1	0.3	<0.1	1.4	1.4	0.36	9.2	0.07	0.40	0.5
	Whole-rock content	12.6	2.19	6.11	0.907	5.8	0.828	10.4	3.4	0.71	23	0.2	30.2	3.2
	Ion-exchangeable (ammonium sulfate)	8.09	1.43	3.56	0.43	2.47	0.34	n.a.	<0.002	<0.02	0.29	<0.06	0.03	0.25
S5	Ion-exchangeable (sodium acetate)	5.29	0.89	2.31	0.27	1.70	0.23	0.024	0.004	0.01	19.8	<0.01	3.5	1.03
	Organic matter	0.88	0.15	0.41	0.053	0.36	0.045	0.161	0.007	0.10	9	0.07	17.7	0.8
	Amorphous Fe oxide and Mn oxide	0.14	0.026	0.064	0.008	0.052	0.006	<0.005	<0.0005	0.01	4.1	<0.1	0.15	0.06
	Fe and Mn oxides	0.05	0.008	0.022	0.003	0.015	<0.0005	<0.005	<0.0005	0.02	1.2	<0.1	0.06	0.07
	Clays and sulfides	0.30	<0.1	0.2	<0.1	0.2	<0.1	<0.1	<0.05	0.07	6.1	0.07	7.4	0.4
	Silicates	0.4	<0.1	0.3	<0.1	0.4	<0.1	1.3	0.1	0.27	6.9	0.07	1.1	0.5
	Whole-rock content	8.54	1.60	4.46	0.690	4.28	0.608	9.3	2.8	0.62	27	0.3	36.8	4.2
	Ion-exchangeable (ammonium sulfate)	4.88	0.90	2.23	0.27	1.51	0.21	n.a.	<0.002	<0.02	9.0	<0.06	0.31	0.71
S6	Ion-exchangeable (sodium acetate)	9.61	1.62	4.27	0.49	2.96	0.40	0.042	0.009	0.02	14.1	<0.01	3.0	0.90
	Organic matter	1.1	0.18	0.50	0.066	0.41	0.053	0.131	0.007	0.10	7	<0.04	16.1	0.6
	Amorphous Fe oxide and Mn oxide	0.18	0.032	0.084	0.010	0.062	0.008	<0.005	<0.0005	0.01	2.3	<0.1	0.23	0.05
	Fe and Mn oxides	0.064	0.011	0.027	0.003	0.024	0.001	<0.005	<0.0005	0.01	0.82	<0.1	0.07	0.08
	Clays and sulfides	0.31	<0.1	0.2	<0.1	0.2	<0.1	<0.1	<0.05	0.07	5.0	0.06	8.2	0.5
	Silicates	0.5	0.1	0.5	<0.1	0.6	<0.1	1.7	0.3	0.38	9.5	0.08	2.1	0.8
	Whole-rock content	11.8	2.14	5.81	0.851	5.15	0.709	9.5	2.7	0.83	38	0.3	34.2	3.8
	Ion-exchangeable (ammonium sulfate)	9.24	1.67	4.11	0.49	2.75	0.37	n.a.	<0.002	<0.02	5.5	<0.06	0.20	0.66
S7	Ion-exchangeable (sodium acetate)	10.3	1.75	4.59	0.49	2.89	0.38	0.05	0.009	0.02	2.4	<0.01	1.7	0.44
	Organic matter	0.86	0.15	0.40	0.052	0.31	0.04	0.069	0.005	0.10	8	<0.04	9.1	0.3
	Amorphous Fe oxide and Mn oxide	0.31	0.051	0.13	0.015	0.089	0.012	<0.005	<0.0005	0.05	6.7	<0.1	0.27	0.08
	Fe and Mn oxides	0.10	0.017	0.045	0.005	0.035	0.003	<0.005	<0.0005	0.06	1.0	<0.1	0.17	0.12
	Clays and sulfides	0.37	<0.1	0.3	<0.1	0.3	<0.1	<0.1	<0.05	0.12	6.2	0.05	10.7	0.5
	Silicates	0.4	0.1	0.4	<0.1	0.6	<0.1	2	0.5	0.49	11.6	0.08	1.2	0.7
	Whole-rock content	11.7	2.06	5.45	0.774	4.59	0.614	9.3	2.7	1.33	46	0.2	28.6	2.8
	Ion-exchangeable (ammonium sulfate)	10.1	1.80	4.29	0.49	2.58	0.34	n.a.	<0.002	0.03	0.59	<0.06	0.12	0.35

See Tables 2 and 3 for the experiment conditions.
Whole-rock content data are from Murakami and Ishihara (2008).
n.a., not analyzed.

Bulletin of the Geological Survey of Japan, vol. 64 (11/12), 2013

南中国江西省定南県の イオン吸着型希土類鉱の多段階抽出実験から得られた地球化学的特徴

実松健造・昆　慶明

要　旨

中国江西省定南県から採取したイオン吸着鉱5試料と風化花崗岩3試料について、6段階抽出実験及び1段階抽出実験を行った結果を本稿にて報告する. 6段階抽出実験はイオン交換、有機物、非晶質 Fe 酸化物・Mn 酸化物、Fe-Mn 酸化物、粘土・硫化物、珪酸塩のフラクションから構成される. イオン吸着型 REE 鉱床から採取したイオン吸着鉱5試料を酢酸ナトリウム水溶液でイオン交換した結果、抽出された元素濃度は REY(REE+Y)で 174 – 388 ppm (全岩含有量の 43 – 68 %に相当)、Thで 1.1 – 3.5 ppm (3.7 – 9.4 %)、Uで0.44 – 1.0 ppm (14 – 25 %)であった. 同様にイオン吸着鉱を硫酸アンモニウム水溶液でイオン交換した結果、元素濃度は REY で 170 – 346 ppm REY (全岩含有量の 42 – 64 %に相当)、Thで 0.03 – 0.31 ppm (0.1 – 0.8 %)、U で 0.25 – 0.71 ppm (8 – 18 %)であった. イオン交換フラクションは Ce が他の REY に比べ著しく枯渇しており、また HREE と Y は全岩組成に比べて若干枯渇していた. Th は有機物フラクションに主に存在し、粘土・硫化物フラクション及び残渣にも含まれる. U は残渣、珪酸塩、イオン交換、粘土・硫化物、有機物フラクションに幅広く存在する. 鉱床外から採取した風化花崗岩3試料の結果も鉱石の結果と大きく変わらなかったが、REY 含有量またはイオン交換性 REY の割合が鉱石よりも若干低かった.

地質調査研究報告 , 第 64 巻，第 11/12 号 , p. 331-340, 2013

論文 - Article

産総研地下水等総合観測網の歪計を使ったゆっくり地震の断層モデルの推定手法

大谷竜 [1]・板場智史 [2]

Ryu Ohtani and Satoshi Itaba, (2013) A method to estimate fault model of slow slip event using strainmeters of the integrated groundwater observation well network for earthquake prediction of the Geological Survey of Japan, AIST, *Bull. Geol. Surv. Japan*, vol.64, p331-340, 11 figs, 1 table.

Abstract: A method to estimate fault parameters due to slow slip event was developed and tested. The method is based on a grid search to find the fault that minimizes the residual between the calculated and observed strain at strainmeter stations. According to a simulation study, it is shown that the method can retrieve the given fault parameters for the case of homogeneous fault slip while the extent of fault is underestimated and the slip amount is overestimated for inhomogeneous slip distribution cases. However, the area where the slip is relatively large and the moment magnitude of the slow slip event are well retrieved.

Keywords: slow slip event, elastic deformation, strain, borehole strainmeter, fault parameter, grid search method

要　旨

産業技術総合研究所（以下，産総研と呼ぶ）の地下水等総合観測網の歪計を使ってゆっくり地震の断層パラメータを推定する手法を開発し，その精度をシミュレーションにより検証した．この方法は，プレート境界上でゆっくり地震が発生すると仮定して任意のすべり量を与え，各観測点における歪の計算値と観測量との残差二乗和を最小にするように，断層の位置や拡がり，すべり量をグリッドサーチで推定するものである．実際に観測されたゆっくり地震のケースを模したシミュレーションを行った結果，均一なすべり分布を与えた場合には精度よく断層パラメータを推定することができた．一方，不均質なすべりを与えた場合には，推定される断層面の拡がりは実際のものよりも小さく，すべり量は大きくなったが，すべり量の大きな領域に断層面が推定され，モーメントマグニチュードも与えたものと大きくは変わらない結果となった．

1．　はじめに

西南日本に沈み込むフィリピン海プレートの沈み込み帯では，過去マグニチュード 8 クラスの巨大地震が繰り返し発生することが知られている．近年，その巨大地震発生領域よりも深部側で，プレート境界が通常の地震（破壊継続時間が数秒～数分）よりも相当長い時間（1 日程度～数年）かけてすべる現象が多数発見され，それらは「ゆっくり地震（slow slip event）」と呼ばれている（Schwartz and Rokosky, 2007）．例えば，愛知県中央部～長野県南部では，継続時間 1 日～ 1 週間程度のゆっくり地震が繰り返し発生し，ゆっくり地震に伴う地殻変動が，同地域に設置されている気象庁の体積歪計や多成分ボアホール歪計によって検出されている（小林ほか，2006）．また，東海地方，紀伊半島，四国において，様々な時間・空間スケールを持つ多様なゆっくり地震が発見されている（例えば，Ozawa *et al.*, 2002; Hirose and Obara, 2005; 小原，2007）．特に，継続時間が数日程度のゆっくり地震は，大地震直前に発生する可能性があると考えられているプレスリップとよく似た特徴があると指摘されている（例えば．日本地震学会地震予知検討委員会（2007））．こうしたことから，ゆっくり地震の特徴や発生条件を解明することは，大地震の発生を考察する上で極めて重要であると考えられる．

フィリピン海プレートの沈み込み帯で発生する巨大地震である東海・東南海・南海地震の予測を目標として，産総研は2007年以降，愛知県～紀伊半島～四国にかけて新しい地下水等の観測点を整備し（小泉ほか，2009; Itaba *et al*., 2010），その観測結果をホームページ上で公開している（http://www.gsj.jp/wellweb/）．本観測網には多成分ボアホール歪計という非常に高精度で地殻歪の連続観測ができる機器が併設されており，ゆっくり地震の調査が進められているところである．多成分ボアホール歪計は，大学等により展開されてきた傾斜計や伸縮計等といった

[1] 地質情報研究部門（AIST, Geological Survey of Japan, Institute of Geology and Geoinformation）Email: ohtani-ryu@aist.go.jp
[2] 活断層・地震研究センター（AIST, Geological Survey of Japan, Active Fault and Earthquake Research Center）

横坑式の地殻変動連続観測機器や，防災科学技術研究所によって全国に展開されている高感度地震観測網(Hi-net)に併設されているボアホール式傾斜計(加速度計)等に比べて精度がよく(小泉，2010)，地殻変動に関連した，より微小な信号の検出が期待できる．

このように，ゆっくり地震が発生している領域に産総研の観測網のボアホール歪計が多数設置されたことから，ゆっくり地震の断層パラメータを詳細に推定できる可能性が出てきた．大谷ほか(2009)では，本観測網全体でのゆっくり地震の検出能力を調べたが，ゆっくり地震の断層パラメータを推定し，その精度を調査することまではしていなかった．本稿では，簡単なグリッドサーチの方法を用い，ゆっくり地震の断層パラメータがどの程度精度良く推定できるのかを，シミュレーションにより調査した．

2．方法

2.1　ゆっくり地震の断層モデルの推定方法

本稿ではゆっくり地震の断層モデルを歪記録から推定するため，プレート面上ですべりを仮定し，観測値を最もよく説明する断層パラメータやすべり量を二段階のグリッドサーチにより求める．プレート面の形状としては，弘瀬ほか(2007)が求めたフィリピン海プレートのものを使用した．

まず第一段階として，プレート境界面上に20 km×20 km のパッチを緯度，経度それぞれについて，0.1° 間隔で作成した(詳細は大谷ほか(2009)参照)．ある任意のパッチについて，フィリピン海プレートの沈み込みの向きと反対方向のすべり (ここでは N135° E) を 5 mm ~ 500 mm の範囲で 5 mm 毎に与え，半無限弾性体中の断層変位に基づくOkada (1985)の式を使って，各観測点における歪，

$$E_{xx}=\frac{\partial u}{\partial x}\ ,\quad E_{yy}=\frac{\partial v}{\partial y}\ ,\quad E_{xy}=\frac{1}{2}\left(\frac{\partial u}{\partial y}+\frac{\partial v}{\partial x}\right)$$

(ここで，u, vはそれぞれ東西方向，南北方向の変位．x, yはそれぞれ東西，南北方向)の変化を計算する．そうしたあるパッチでのすべりに対して，以下のように各観測点において，この計算値と観測値の残差二乗和Δを計算し，観測点全てについての和を求める．

$$\Delta=\sqrt{\frac{\sum_{i=1}^{N}\left\{(E_{xx(i)}^{Obs}-E_{xx(i)}^{Cal})^2+(E_{xy(i)}^{Obs}-E_{xy(i)}^{Cal})^2+(E_{yy(i)}^{Obs}-E_{yy(i)}^{Cal})^2\right\}}{3N}}$$

ここでNは観測点の数，$E_{xx(i)}^{Obs}$，$E_{xx(i)}^{Cal}$ 等はそれぞれi番目での観測点での歪の観測値，計算値である．これを全てのパッチについて行い，与えたホワイトノイズの 1.5倍以内にΔが収まるものを求め，特にそのうちで最小となるもののパッチをすべりの候補となる断層面の位置とする．なおここで 1.5 倍としたのは，適当なモデルであればΔがホワイトノイズと同程度になることが予想されるが，実際には他のノイズが存在するため，それらを考慮して高めに設定したためである．以上が第一段階である．

次に第二段階として，候補となるパッチとその周辺において，断層面の大きさを変えて，断層パラメータやすべり量の推定を行う．即ち，それぞれのパッチにおいて，断層の幅・長さをそれぞれ 10 km ~ 80 km まで 5 km毎に変え，それぞれの組み合わせに対して 5 mm ~ 500 mm のすべり量を与えて，残差を計算した．これらの内，最も残差が小さくなる組み合わせのものを最終的な推定値として決定した．またその推定値を中心として各パラメータの値を変えて，計算されたΔが，与えたホワイトノイズの 1.5倍以内に収まる値の範囲を求められたパラメータの幅とした．

2.2　シミュレーションによる評価

この手法による断層すべり推定精度の評価のため，以下の方法でシミュレーションデータを使った解析を行った．まず，設定した断層面で任意のすべり量を与え，観測点でどのくらいの歪が発生するのかを計算した．本稿では実際のケースと似せるため，本稿では紀伊半島で発生するゆっくり地震に擬した仮想的なゆっくり地震のシミュレーションを行った．観測点としては，第 1 図の赤枠で囲った領域にある 5 点を使用する．まず，断層モデルとして，第 2 図のような一様なすべりモデル(ケースA)を想定した．ここで想定した断層モデルから計算される各観測点での歪を「観測値」として使用する．またすべり分布が一様な場合のみでなく，第 3 図のようにガウス関数状の分布を持つような不均質な場合(ケースB)も想定した．ここで想定した断層モデルから計算される各観測点の歪を「観測値」として使用する．次に，観測点での模擬時系列を計算するために，すべりの継続時間を 2 日間として，最終的な累積すべり量の分布が一様なすべりの場合は第 2 図，一様でないすべりの場合は第 3 図となるようなすべりを与えた．一様でないすべりの場合について，断層面上のすべりの時間発展を第 4 図に示す．これにノイズを加えて歪 *Exx*, *Exy*, *Eyy*の各成分の時間値データを生成した(第 5 図)．観測点の平均的なノイズとして，観測点の大半を占める石井式歪計のデータの24時間階差(降雨時期除く)のばらつきを参考に(松本・北川，2005)，今回若干大きめの 0.5×10^{-8} の標準偏差を持つホワイトノイズで数値計算による検証を行った．こうして生成された 3 日間のデータの，最初の半日と最後の半日のそれぞれの平均の差から得られた主歪を第 6 図，第 7 図に示す．この模擬データを使って，与えられた断層面やすべり分布をどの程度推定できるかを見た．データのSN比の影響を見るため，すべり量を1/2にした場合のケースについても同様の解析を行った．

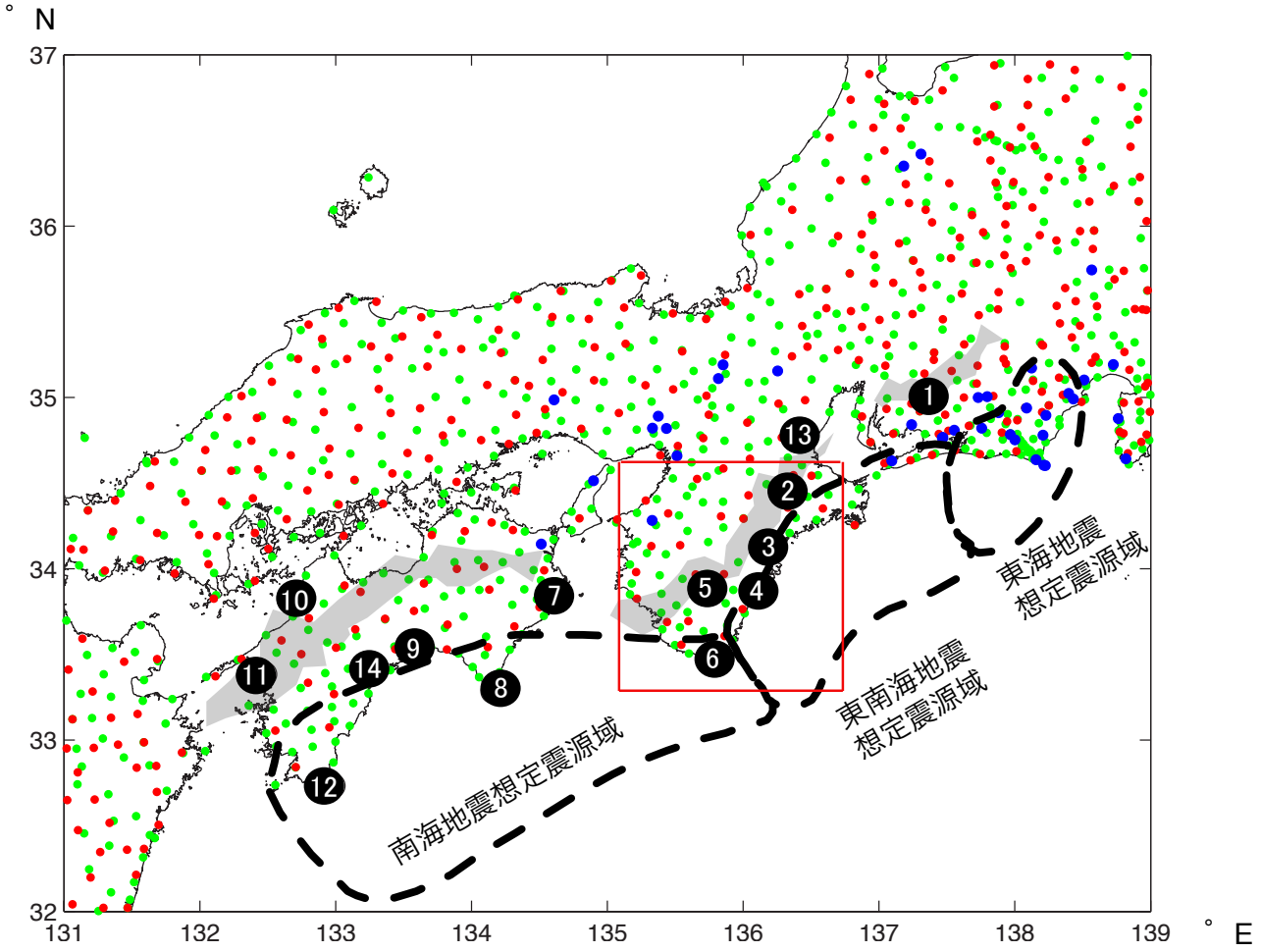

第１図　産総研の地下水等総合観測網の新規観測点分布（数字のついた黒丸：観測点の名称は第1表を参照）．赤点は防災科学技術研究所の高感度地震観測網Hi-netの観測点，緑点は国土地理院のGNSS連続観測網GEONETの観測点，青点は既存のボアホール歪計の観測点（いずれも地震調査研究推進本部のホームページより：http://www.jishin.go.jp/main/p_chousakansoku01.htm）．薄い灰色の領域は，ゆっくり地震が頻発に発生している領域（小原(2007)より）．赤線で囲われた領域が本論で解析した領域．

Fig. 1　Location of the new observation sites of the integrated groundwater well network for earthquake prediction of the Geological Survey of Japan, AIST (numbers with black circles; the names of the stations are summarized in Table 1). The red dots represent the Hi-net seismograph stations of the National Research Institute for Earth Science and Disaster Prevention (NIED), the green dots represent the GEONET GNSS stations of the Geospatial Information Authority of Japan (GSI), and the blue dots represent stations of borehole strainmeters (quoted from the web page of the Headquaters for the Earthquake Research Promotion: http://www.jishin.go.jp/main/p_chousakansoku01.htm). The shaded regions represent the area where slow slip events are frequently observed (Obara (2007)). The red box indicates the study area.

第１表　産総研の新規観測点とその記号

Table. 1　Name of the new AIST observation sites and the abbreviation.

①	豊田神殿 (TYS)	⑧	室戸岬 (MUR)
②	松阪飯高 (ITA)	⑨	高知五台山 (KOC)
③	紀北海山 (MYM)	⑩	松山南江戸 (MAT)
④	熊野井内浦 (ICU)	⑪	西予宇和 (UWA)
⑤	田辺本宮 (HGM)	⑫	土佐清水松尾 (TSS)
⑥	串本津荷 (KST)	⑬	津安濃 (ANO)
⑦	阿南桑野 (ANK)	⑭	須崎大谷 (SSK)

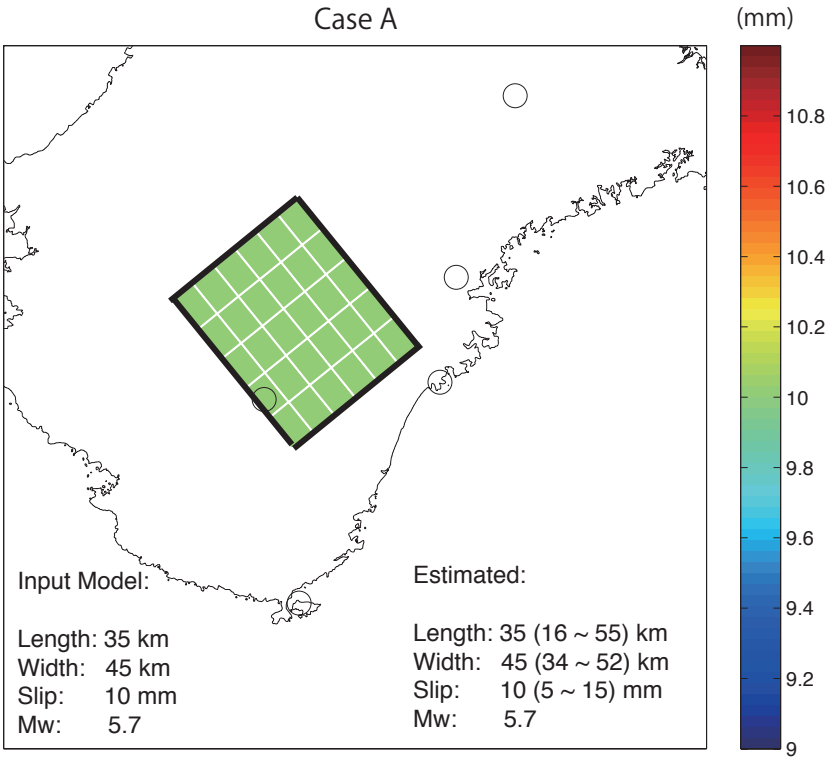

第２図　与えられた仮想的な断層すべりの空間分布（色のついたパッチ）と，推定された断層面の位置（太い黒線で囲まれた領域）．仮想的な断層すべりのパラメータはInput Trueに，推定された断層パラメータはEstimatedに示す．Estimatedの括弧内の数値は，推定値の不確実性（詳しくは本文を参照）．本ケースの場合は，均一なすべり分布である．

Fig. 2　Distribution of hypothetical fault slip (colored patches) and estimated fault plane (thick black rectangular). The fault parameters are shown on the bottom. The uncertainty of the estimated parameters are also indicated in the parenthesis. In this case, slip distribution is homogeneously given.

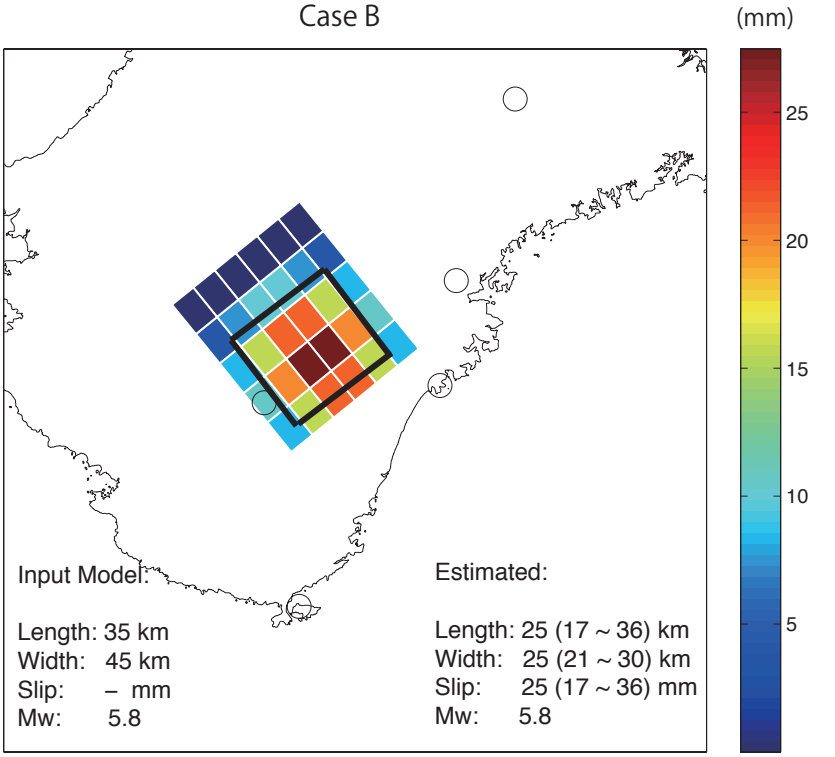

第3図　第2図と同じ．但し不均一なすべり分布を与えている．

Fig. 3　Same as Fig. 2 but the amount of slip is heterogeneously given.

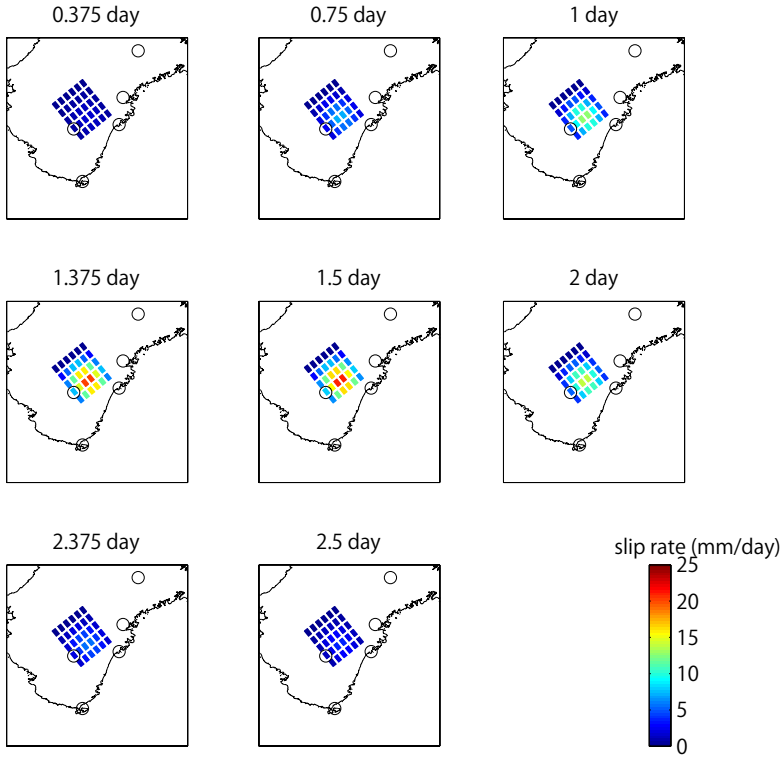

第4図　第3図で与えられた仮想的な断層面上のすべり速度の時空間変化.

Fig. 4　Spatio-temporal variation of the slip rate on the hypothetical fault given in Fig. 3.

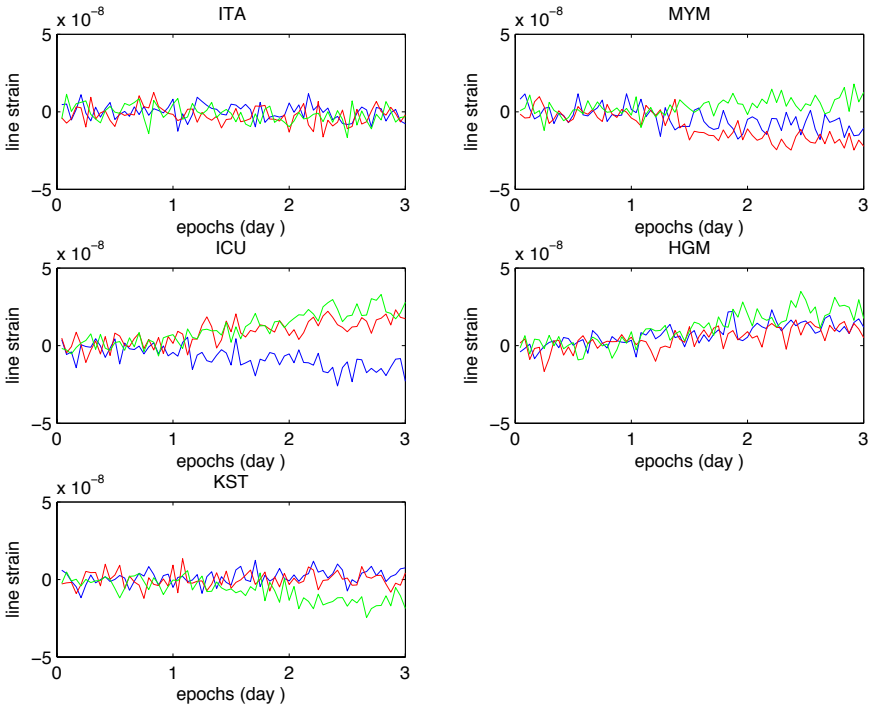

第5図　産総研観測点における，第4図のすべりによって生成された線歪の時系列．青，赤，緑の線はそれぞれ *Exx*, *Exy*, *Eyy*の歪を示す．ノイズレベルを 0.5×10^{-8} とした.

Fig. 5　Synthetic time series of line strain due to the fault slip given in Fig. 4 for AIST stations. Blue, red, and green lines indicate *Exx*, *Exy*, and *Eyy* components, respectively. Noise level is assumed to be 0.5×10^{-8} .

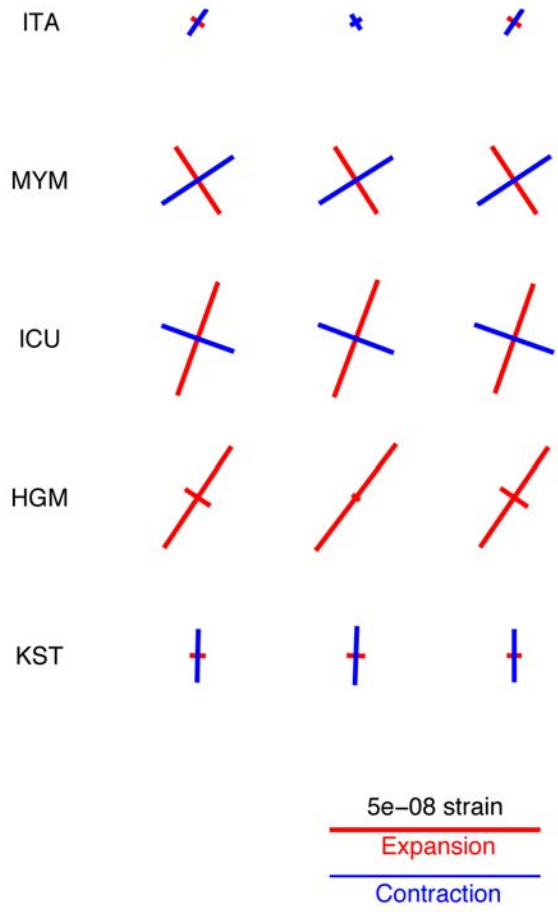

第6図　第2図の均質なすべり分布によってもたらされる産総研観測点での主歪．左から右へ，与えられた断層すべりによる真の主歪，生成された疑似時系列から計算されたもの，本手法で推定された断層モデルを用いて計算されたもの．

Fig. 6　Principal strain at the AIST stations. From left to right, strains calculated for the fault slip given in Fig. 2, derived from the corresponding synthetic time series, and estimated using the fault parameters determined by the grid search, are shown.

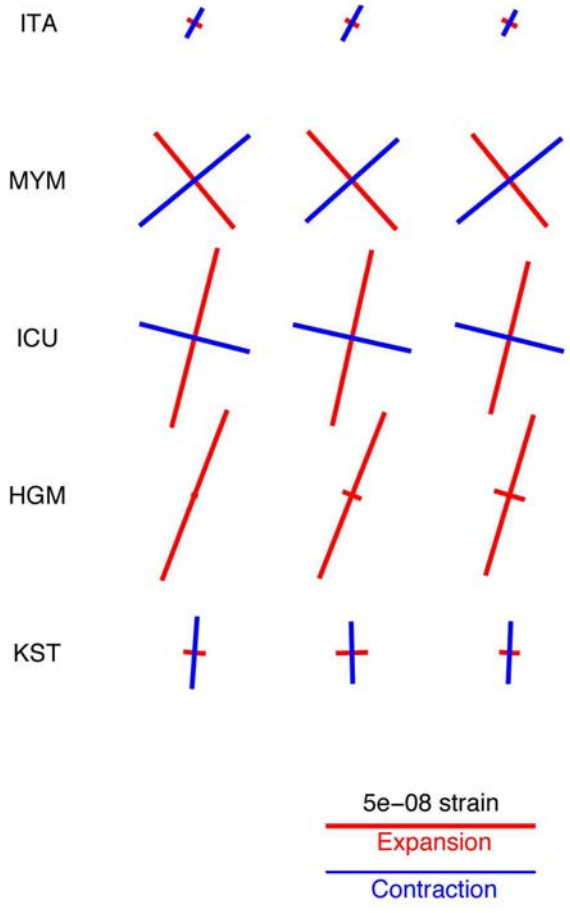

第7図　第6図と同じ，但し第3図の不均質なすべり分布の場合．

Fig. 7　Same as Fig. 6 but for the slip case in Fig. 3.

3. 結果と考察

第 8 図，第 9 図に，第一段階として絞られた断層すべりの候補位置とすべり量を均質すべり分布(ケースA)，不均質すべり分布(ケースB)のそれぞれのケースについて示す．なお，ここでは計算時間短縮のため，使用するパッチはゆっくり地震が発生していると推定されている，深さ20 km ～ 40 kmのものに限定している．太い赤線で囲まれた四角が，グリッドサーチにより得られた推定位置である．更に，Δが，与えられたホワイトノイズの1.5 倍以内に収まるパッチがあれば，細い赤線の四角で囲われる(第11図を参照)．グレースケールは，各パッチで，上記のように計算されたΔの中で最小のものを示しており，濃いパッチが残差の小さいものである．与えられた断層付近に候補が求められており，その候補の周囲は残差が小さいことが分かる．残差が小さい領域がやや西側に広がることについては，観測点配置の偏りによるものと考えられる．次に，残差が最小のパッチとその周辺で，断層の大きさを変えながら同様の計算を行い，最も残差が小さくなった断層の幅，長さ，すべり量の組み合わせを求めた．最終的に求められた断層パラメータを第 2 図，第 3 図の黒線に示す．

均質すべりの場合(ケースA)については，与えられた断層パラメータと非常に近い値が得られていることが分かる．但し，パラメータの幅は大きなものになっている．例えば均質なすべりのケースの場合，長さで ±20 km 程

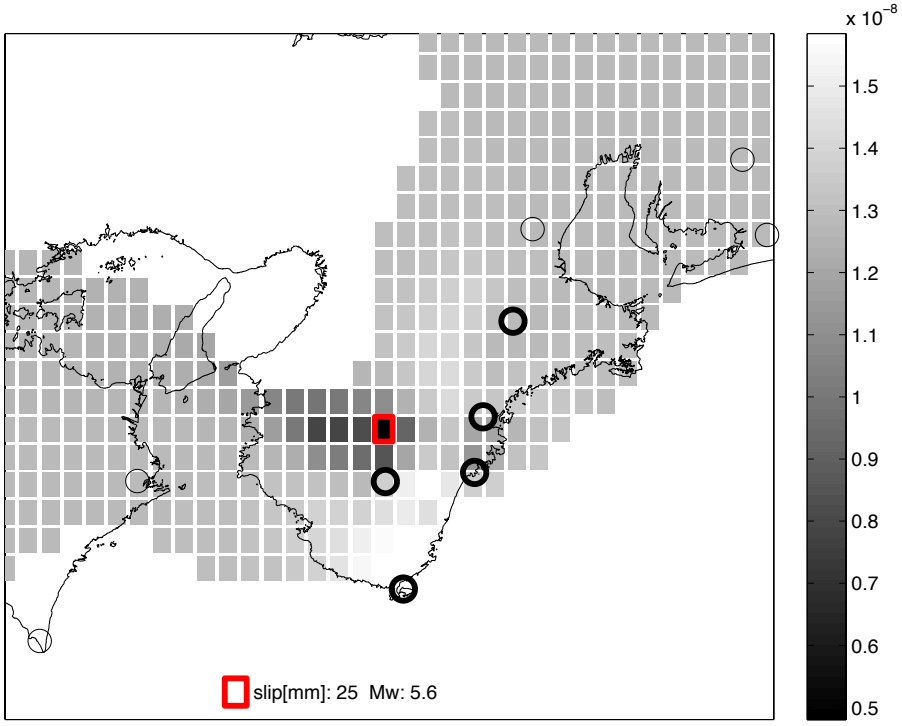

第8図　本手法の第一段階で推定された暫定的な断層すべりの候補の位置と滑り量．色の濃淡は残差量を示す．第2図の断層すべりのケースの場合．

Fig. 8　Tentative fault plane and slip amount estimated as the first step by the grid search for the case in Fig. 2. The small rectangular patches are faults and the gray color indicates the residual of fit.

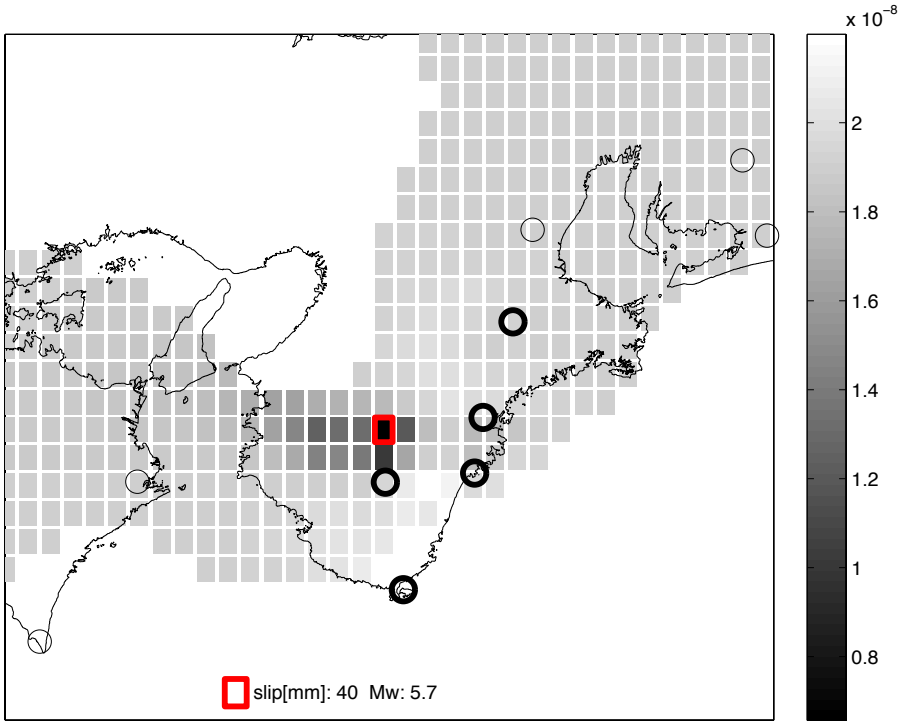

第9図　第8図と同じ．但し断層すべりは第3図の場合．

Fig. 9　Same as Fig. 8 but for the slip case in Fig. 3.

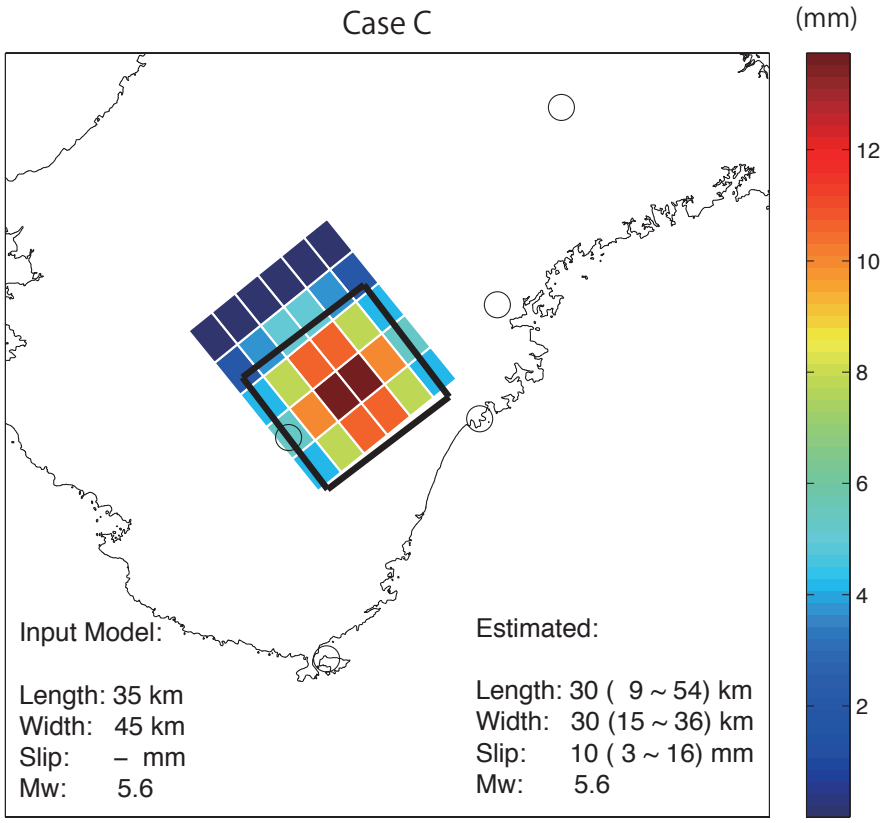

第 10 図　第 3 図と同じ．但し全体のすべり量を半分に小さくした場合．

Fig. 10　Same as Fig. 3 but the slip amount is reduced to a half.

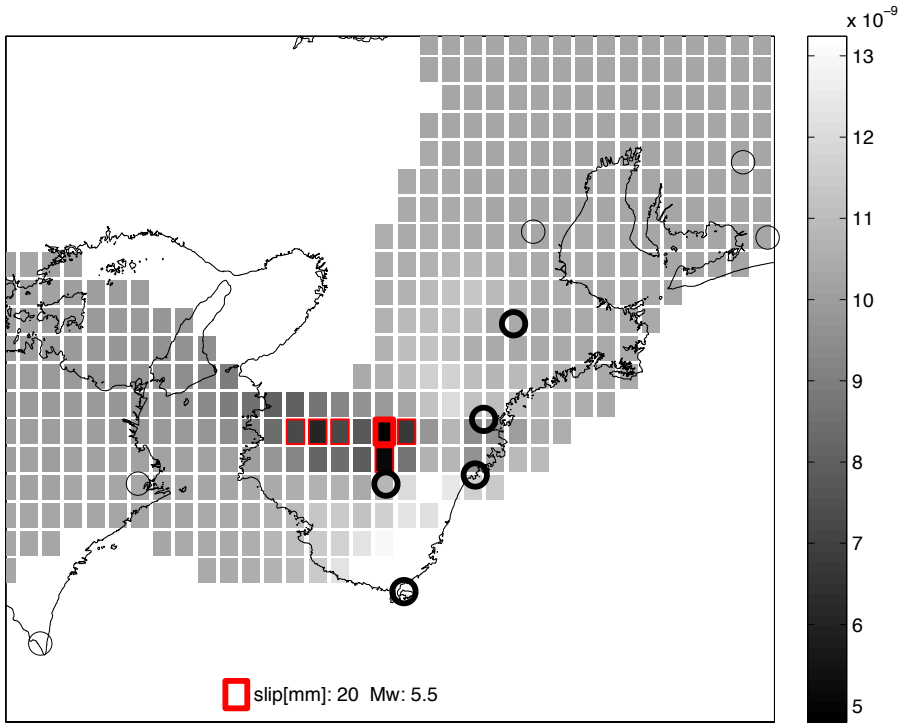

第 11 図　第 8 図と同じ．但し断層すべりは第 10 図の場合．

Fig. 11　Same as Fig. 8 but for the slip case in Fig. 10.

度，すべり量も半分から 1.5 倍程度の不確実性がある．疑似データ作成の際のホワイトノイズの生成状態の影響を見るために，何度かシミュレーションを試みたが，傾向は変わらなかった．

不均質なすべりの場合（ケースB）では，与えられた断層面よりも狭い範囲に推定されているが，求められたすべり量は与えられたすべり量の平均よりも大きく，結果，モーメントマグニチュードは同じ程度の大きさに推定されていることが分かる．この断層パラメータを用いて計算された各観測点での主歪を第 6 図，第 7 図の右側に示す．観測値（真ん中）をよく説明できており，また真の値とよく似ていることが分かる．

不均質なすべりの場合（ケースB）について，すべり量を1/2にして（ケースC）同様の解析を行った結果を第10図，第11図に示す．このケースでは，観測点配置の偏りに加えて，SN比が小さいためか，第 1 段階として推定される断層位置は複数の候補が推定されている．また，最終的に推定される断層面の拡がりは，ケースBと同じように与えられたすべり域よりも小さくなっている．しかし信号の大きさが半分になっているにも関わらず，主要なすべり域を検出できていることは注目される．推定されたすべり量は，与えられたすべり量の平均よりも大きくなっている傾向が見られるものの，モーメントマグニチュードに着目すると，推定値と入力値は同程度である．以上の結果から，本手法は，ゆっくり地震の主要なすべり域やマグニチュードをよく推定できていると言える．

但し，推定されたパラメータにはある程度の幅があり，推定結果の解釈においては注意しなければならない．ゆっくり地震は，地殻変動として検出されている以外にも，微動として地震計による記録からも検出されているが，ゆっくり地震の断層面の拡がりについては，微動を伴わないでゆっくりとしたすべりが発生しているかどうか論点となっており（例えばHirose and Obara (2010)），ゆっくりとしたすべりの領域が微動の発生している範囲のみで起きているのか，あるいは更に大きく広がっているのか判断するには，注意が必要となるであろう．

その一方，本手法では一様なすべりを仮定しているにせよ，ガウス関数状に不均質に分布するすべりが存在した場合でも，すべりの大きな領域に断層面が推定できていること，及び最終的に求められるモーメントマグニチュードも大きく違っていないことは注目に値する．これまで気象庁のゆっくり地震推定で使用されていたアルゴリズムである中村・竹中(2004)の方法でも，同じくグリッドサーチを用いたゆっくり地震の推定を行っているが，彼らの手法ではすべりと断層の大きさの間に通常地震の経験式を使用している．しかし，ゆっくり地震のそれは，通常地震のものとは大きく異なると言われている(例えば，Sekine *et al*., 2010)．そうした物理的な仮定を置いていない本手法はそれゆえ，より一般性が高く，汎用性の高い断層モデルの推定ができると期待される．

謝辞：気象研究所弘瀬冬樹氏には論文中のプレート等深線データを提供いただきました．地下水等総合観測網の観測点設置において産総研，地方自治体を始め多くの関係者の協力を得ています．また，本論の手法開発においては，活断層・地震研究センター地震地下水チームの北川有一氏・松本則夫氏・高橋誠氏・小泉尚嗣氏との議論から大変貴重な助言をいただきました．匿名の査読者には有意義なコメントを頂きました．ここに記して感謝します．

文献

弘瀬冬樹・中島淳一・長谷川昭 (2007) Double-Difference Tomography法による西南日本の 3 次元地震波速度構造およびフィリピン海プレートの形状の推定, 地震 2, 60, 1-20.

Hirose, H., and K. Obara (2005), Repeating short- and long-term slow slip events with deep tremor activity around the Bungo Channel region, southwest Japan, *Earth Planets Space*, 57, 961–972.

Hirose, H., and K. Obara (2010), Recurrence behavior of short-term slow slip and correlated nonvolcanic tremor episodes in western Shikoku, southwest Japan, *J. Geophys. Res*., 115, B00A21, doi:10.1029/2008JB006050.

Itaba, S., N. Koizumi, N. Matsumoto, and R. Ohtani (2010) Continuous Observation of Groundwater and Crustal Deformation for Forecasting Tonankai and Nankai Earthquakes in Japan, *Pure Appli. Geophys*.,167, 1105–1114.

小林昭夫・山本剛靖・中村浩二・木村一洋 (2006) 歪計により観測された東海地域の短期的スロースリップ（1984 ～ 2005 年）, 地震 2, 59, 19-27.

小泉尚嗣, 高橋誠, 松本則夫, 佐藤努, 大谷竜, 北川有一, 板場智史, 梅田康弘, 武田直人, 重松紀生, 桑原保人, 佐藤隆司, 今西和俊, 木口努, 関陽児, 塚本斉,山口和雄, 加野直巳, 住田達哉, 風早康平, 高橋正明, 高橋浩, 森川徳敏, 角井朝昭,下司信夫, 中島隆, 中江訓, 大坪誠, 及川輝樹，干野真，東南海・南海地震予測のための地下水等総合観測点整備について（2009）地質ニュース，662，6-10.

小泉尚嗣（2010）地下水位観測による地殻変動の推定-現状と展望- 地震ジャーナル, 50, 89-94.

松本則夫・北川有一 (2005) 想定東海地震震源域付近の観測井における地下水位の歪感度とノイズレベル，測地学会誌，51，131-145.

中村浩二・竹中潤 (2004) 東海地方のプレート間すべり推

定ツールの開発，験震時報，68，25-35.
日本地震学会地震予知検討委員会 (2007) 地震予知の科学, 東京大学出版会，227pp.
小原一成 (2007) 深部低周波微動に同期する短期的スロースリップイベントの検出－防災科研Hi-net傾斜観測による成果－，測地学会誌, 53, 25-34.
大谷竜・板場智史・北川有一・佐藤努・松本則夫・高橋誠・小泉尚嗣 (2009) 産総研地下水等総合観測網による東南海・南海地震の仮想的プレスリップの検出能力の評価, 地質調査研究報告，60, 11/12，511-525.
Okada, Y. (1985) Surface deformation due to shear and tensile faults in a half-space, *Bull. Seism. Soc. Am*., 75, 1135-1154.
Ozawa, S., M. Murakami, M. Kaidzu, T. Tada, Y. Hatanaka, H. Yarai, and T. Nishimura (2002) Detection and monitoring of ongoing aseismic slip in the Tokai region, central Japan, *Science*, 298, 1009 – 1012.
Schwartz, S., and J. Rokosky (2007) Slow slip events and seismic tremor at circum-Pacific subduction zones, Reviews of Geophysics, 45(3), doi:10.1029/2006RG000208.
Sekine, S., H. Hirose, and K. Obara (2010) Along-strike variations in short-term slow slip events in the southwest Japan subduction zone, *J. Geophys. Res*., 115, B00A27, doi:10.1029/2008JB006059.

（ 受 付：2013 年 8 月 19 日； 受 理：2013 年 12 月 17 日 ）

地質調査研究報告　第 64 巻　(第１号－第１２号)

CONTENTS OF VOLUME 64

本年掲載論文の査読を下記の方々にお願いいたしました．記して厚くお礼申し上げます．

西岡芳晴・御子柴真澄・宮崎一博・鎌田祥仁（筑波大学）・上岡　晃・行谷佑一・佐脇貴幸・内藤一樹・小松原 琢・及川輝樹

地質調査総合センター研究資料集

574	第 10 回水文学的・地球化学的手法による地震予知研究についての日台国際ワークショップ予稿集	謝　正倫・小泉尚嗣・松本則夫　編
575	第 11 回水文学的・地球化学的手法による地震予知研究についての日台国際ワークショップ予稿集	小泉尚嗣、松本則夫、謝　正倫　編
576	第 1 回アジア太平洋大規模地震・火山噴火リスク対策 (G-EVER) シンポジウム講演要旨集	宝田晋治・石川有三・小泉尚嗣・内田利弘・桑原保人・高田亮・吾妻　崇・田村　亨・古川竜太・吉見雅行　編
577	地質情報展 2012 おおさか　ー過去から学ぼう大地のしくみー	川畑　晶・中島和敏・大熊洋子・百目鬼洋平　編
578	第 3 回火山巡回展霧島火山ーボラ（軽石）が降ってきた！新燃岳の噴火とその恵みー	及川輝樹・筒井正明・田島靖久・芝原暁彦・古川竜太・斎藤元治・池辺伸一郎･佐藤　公･小林知勝･下司信夫・西来邦章・東宮昭彦・宮城磯治・中野　俊・渡辺真人
580	十和田火山御倉山溶岩ドームの反射電子像	宮城磯治・工藤　崇
581	第 3 回火山巡回展　霧島火山ーボラが降ってきた！新燃岳の噴火とその恵みー資料映像「霧島火山新燃岳 2011 年噴火」	芝原暁彦・及川輝樹
582	非常に古い地下水年代測定のための日本列島の帯水層岩石を対象にしたヘリウム同位体生成速度および放射性塩素同位体放射平衡値データ集	森川徳敏・戸崎裕貴
583	第 1 回アジア太平洋大規模地震・火山噴火リスク対策 (G-EVER) シンポジウムプロシーディングス	宝田晋治・石川有三・小泉尚嗣・内田利弘・桑原保人・高田　亮・吾妻　崇・重松紀生・田村　亨・丸山　正・安藤亮輔・古川竜太・吉見雅行　編
584	地質標本館特別展「地球の恵み地熱・地中熱エネルギーを活用しよう」	石戸恒雄・唐澤廣和・水垣桂子・大熊茂雄・阪口圭一・佐脇貴幸・杉原光彦・高倉伸一・内田洋平・柳澤教雄・安川香澄・吉岡真弓
585	いわき地域重力探査データ	村田泰章・松本　陽・岡田　力・高橋美江
586	日本列島の地殻温度構造と粘弾性構造の 3 次元モデルおよび地殻活動シミュレーションに関する数値データ	長　郁夫・桑原保人
587	地質情報展 2013 みやぎ　ー大地を知って明日を生かすー	吉田清香・澤井祐紀・川畑　晶

地質調査総合センターの最新出版物

200 万分の 1 地質編集図	No. 4	日本地質図（第 5 版）
	No. 11	日本の火山（第 3 版）
20 万分の 1 地質図幅	伊勢・静岡及び御前崎（第2版）・与論島及び那覇・八代及び野母崎の一部・新潟（第2版）	
5 万分の 1 地質図幅	足助・京都東南部・新居浜・青森西部・今庄及び竹波・早池峰山	
海外地球科学図	アジア地質図（1:500 万）	
	中央アジア鉱物資源図（1:300 万）	
海洋地質図	No. 81	日高舟状海盆表層堆積図 （1:20 万）
	No. 82	奥尻海盆表層堆積図 （1:20 万）
構造図	No. 14	全国主要活断層活動確率地図
火山地質図	No. 1	桜島火山地質図（第 2 版）（1:3 万）
	No. 16	十勝岳火山地質図（1:3 万）
	No. 17	諏訪之瀬島火山地質図（1:3 万）
鉱物資源図	No. 7	南西諸島（1:50 万）
特殊地質図	No. 39	千葉県清和県民の森周辺の地質図
重力図	No. 29	姫路地域重力図（ブーゲー異常）
	No. 30	徳島地域重力図（ブーゲー異常）
	S3	甲府地域重力構造図（ブーゲー異常）
空中磁気図	No. 44	岩手火山地域高分解能空中磁気異常図
	No. 45	福井平野地域高分解能空中磁気異常図
数値地質図	G-16	20 万分の 1 日本シームレス地質図 DVD 版
	G-17	九州地質ガイド
	FR-2	燃料資源地質図「東部南海トラフ」
	GT-4	全国地熱ポテンシャルマップ
	S-2	海陸シームレス地質情報集「新潟沿岸域」 DVD 版
	S-3	海陸シームレス地質情報集「福岡沿岸域」 DVD 版
	V-3	口永良部島火山地質データベース
	P-2	日本重力データベース DVD 版
	G20-1	20 万分の 1 数値地質図幅集「北海道北部」第 2 版
	G20-2	20 万分の 1 数値地質図幅集「北海道南部」第 2 版
	E-5	表層土壌評価基本図 ～富山県地域～
その他	日本の熱水系アトラス	
	海と陸の地球化学図	

地質調査研究報告 第64巻 第11/12号
平成25年12月27日　発行

独立行政法人 産業技術総合研究所
地質調査総合センター
〒305-8567 茨城県つくば市東1-1-1
つくば中央第7

Bulletin of the Geological Survey of Japan
Vol.64 No.11/12 Issue December 27, 2013

National Institute of Advanced Industrial
Science and Technology
Geological Survey of Japan
AIST Tsukuba Central 7, 1-1, Higashi 1-chome,
Tsukuba, Ibaraki 305-8567 Japan

AIST13-G68686

Online ISSN : 2186-490X
Print ISSN : 1346-4272
CODEN : CCKHA7

地質調査研究報告

BULLETIN OF THE GEOLOGICAL SURVEY OF JAPAN

Vol. 64 No. 11/12 2013

CONTENTS

GEOLOGICAL SURVEY OF JAPAN
National Institute of Advanced Industrial Science and Technology

1-1, Higashi 1-chome, Tsukuba, Ibaraki, 305-8567 Japan

地 調 研 報
Bull. Geol. Surv. Japan
Vol. 64, No. 11/12, 2013

Bulletin of the Geological Survey of Japan

Vol. 64, No. 11/12, P. 313–340 2013